ARC FAR SIDE IMPACT
COLLABORATIVE RESEARCH PROGRAM
TASK 2: BIOMECHANICAL TEST PROGRAM

FINAL REPORT

Prepared by
Frank A. Pintar, Medical College of Wisconsin
Jason Moore, Medical College of Wisconsin

Contributing Authors
Narayan Yoganandan, Medical College of Wisconsin
Brian D. Stemper, Medical College of Wisconsin
Kennerly Digges, George Washington University
Ola Bostrom, Autoliv AB
Stephen W. Rouhana, Ford Motor Company
Brian N. Fildes, Monash University

ABSTRACT

Injury to the far side occupant has been demonstrated as a significant portion of the total trauma in side impacts. The objective of the study was to determine the response of PMHS in far side impact configurations, with and without generic countermeasures, and compare responses to the WorldSID and THOR dummies. A far side impact buck was designed for a sled test system that included a center console and three-point belt system. The buck allowed for additional options of generic countermeasures including shoulder or thorax plates or an inboard shoulder belt. The entire buck could be mounted on the sled in either a 90-degree (3-o'clock PDOF) or a 60-degree (2-o'clock PDOF) orientation. A total of 18 tests on six PMHS were done to characterize the far side impact environment at both low (11 km/h) and high (30 km/h) velocities. WorldSID and THOR-NT tests were completed in the same configurations to conduct matched-pair comparisons. For high-speed tests, center console pelvic forces ranged from 3 to 5 kN; thorax or shoulder plate forces (when present) ranged from 3 to 4 kN. Shoulder belt forces were highly dependent on the presence of a thorax or shoulder restraint; without alternate restraint, both inboard and outboard shoulder belt forces were approximately 3 kN. Both dummies had positive and negative biofidelity outcomes. For example, the THOR shoulder against a side restraint produced much higher forces than the PMHS or WorldSID; the WorldSID produced greater pelvic loads in the presence of a shoulder plate than the PMHS or THOR. Both dummies provided good measures of head excursion compared to PMHS across most configurations. Both dummies had difficulty measuring appropriate chest deformations due to belt loading because of measurement device locations. Considerations for countermeasure design should account for the potential for increased injuries to other body regions. For example, in the PMHS tests, a high inboard shoulder belt configuration produced carotid artery trauma. The far side impact environment is unique and there are currently no dummies that are designed specifically to assist countermeasure design. The current test series demonstrated that with some modifications, both the WorldSID and THOR have the potential to function as good human surrogates in far side impact configurations.

KEYWORDS

Biomechanics, Far Side Impacts, Biofidelity, Dummy testing, Post Mortem Human Subjects

1 INTRODUCTION

Side impact crashes are second only to frontal impacts in frequency. In general, the severity of injury, for side impacts, however, is greater than for frontal impacts [Banglmaier et al. 2003; Frampton et al. 1998; Franklyn et al. 1998; Haland et al. 1990; Yoganandan et al. 2000]. When a side impact occurs to the opposite side of an occupant's seating location it is termed a far side crash or a non-struck side crash. In a study using NASS/CDS data from 1993-2002, far side impact AIS=3+ trauma was found to be 43% of the total trauma in side impacts [Gabler et al. 2005]. The chest (33%) followed by the head (27%) were the most likely body regions to suffer serious injury in far side crashes. In another study of US far side crashes, chest and abdominal injuries tended to occur in lower severity crashes while head injuries predominated in higher severity crashes [Augenstein et al. 2000]. Adding fatalities and MAIS=3+ injuries Digges et al. (2005) attributed 42% Harm [Malliaris et al. 1982] to the head and 41% Harm to the trunk for belted far side impact occupants and 55% head and 30% trunk Harm for unbelted far side occupants.

A distribution of far side crash injury by principal direction of force (PDOF) was collapsed down to every clock direction; both 60 +/- 15 degrees and 90 +/- 15 degrees were prominent crash directions [Gabler et al. 2005]. In a preliminary experimental investigation using a vehicle test, it was determined that a common cause for head injury is contact with the opposite side door or B-pillar [Fildes et al. 2002]. Torso trauma occurs commonly to the internal organs such as the liver and spleen and has been largely attributed to belt loading [Augenstein et al. 2000; Yoganandan et al. 2000]. Current belt systems were not designed for protection in far side crashes and observations from real-world crashes indicate that the occupants slipped out of the shoulder belt approximately 35% of the time [Mackay et al. 1991].

Countermeasures designed specifically for far side impacts are few. Belt positioning and belt geometry as well as limiting thoracic excursion may be methods of enhancing the protection to far side crash occupants. Newer belt technologies such as pre-tensioners and belt positioning systems may provide some inherent protection to far side crash occupants if these belt systems reduce the potential for belt slip and limit head excursion.

Before specific countermeasures can be designed or tested, an appropriate anthropomorphic test device (ATD) should be identified for the far side impact mode. Since there is currently no ATD specifically designed for far side impacts, and since the biofidelity requirements for far side impact have not been established, the current investigation was conducted as a first step. The objectives of the present study, therefore, were to determine responses of post mortem human subjects (PMHS) in far side impact configurations, with and without generic countermeasures and to compare responses with two possible candidate ATDs.

2 METHODS

A far side impact buck was designed for a sled test system that included, as a standard configuration, a center console and outboard three-point belt system. This configuration assumed a left side driver with a right side impact. The geometry and dimensions are shown in Figure 1. The buck allowed for additional options of generic (not linked to any manufacturer's product) restraints including shoulder or thorax restraint or an inboard shoulder belt. The entire buck could be mounted on the sled in either a 90-degree (3-o'clock PDOF) or a 60-degree (2-o'clock PDOF) orientation. The center console was composed of a vertically oriented pelvis plate and a horizontally oriented center console plate. The pelvis plate was designed such that the entire hip engaged the plate; the top of the plate was slightly higher than the lateral iliac crest of a 50th percentile male. The fore-aft dimension for the center console plate was determined as the dividing point on the Hybrid-III dummy between the hip and thigh junction when the dummy sat in the seat. The lower belt anchor point was determined using the Hybrid-III 50th male dummy and positioning the lap belt such that the belt traversed a 45-degree angle from pelvis to anchor point. Upper belt anchor points were adjustable as described later. The console plate was padded with 25 mm of 207 kPa (30 psi) paper honeycomb. If either a thorax restraint plate or shoulder restraint plate was used, the padding was 25 mm of 103 kPa (15 psi) paper honeycomb. The dimensions of the shoulder or thorax plates were 100 mm in height and 460 mm in length.

As listed in Table 1, eighteen different far side test conditions were evaluated including inboard belt geometry, and shoulder or thorax restraints. Some configuration ID's are missing because these tests were part of a larger series; configurations that were not tested with a PMHS are not included. A larger WorldSID test series has been previously published [Pintar et al. 2006]. To aid in the presentation of results, a figurine unique to each test configuration is presented (Figure 2). Each figurine depicts test velocity, test angle, if a thorax or shoulder plate was used, and position of shoulder belt (high, low, inboard, outboard) and if pre-tension was applied.

All tests were conducted with a lap belt, a center console, and either an inboard or outboard shoulder belt. The shoulder and lap belts were low-elongation standard belts (6% elongation at 11.1 kN). The shoulder belt could be configured such that the D-ring anchor point was horizontal with the top of the shoulder (low position), 90 mm above the shoulder (mid position), or 150 mm above the shoulder (high position). All of these D-ring locations were approximately 120 mm behind the mid point of the shoulder. As a realistic worst-case configuration, the shoulder belt D-ring could be positioned in the mid position vertically, and forward (30 mm behind shoulder instead of 120 mm behind) of the usual anchor location (Configurations 10-11). Tests were conducted at either a direct 90 degree impact or an oblique 60 degree direction and low speed (11 km/h) or high speed (30 km/h) delta-v. Test speeds were chosen based upon real-world data from Gabler et al. (2005) that indicated at 11 km/h less than 5% of the cumulative serious injuries occurred, and at 30 km/h just over 50% of the cumulative serious injuries occurred. Thus, low speed tests were designed to provide low-level response data without injuries and high speed tests were designed to provide responses where countermeasures would be designed. The high speed test condition was a 100 ms square wave sled pulse with 8.8 *g* average acceleration using a bungee cord propelled rebound sled (MTS Systems, Minneapolis, MN). The low speed test was approximately a 60 ms pulse with 5.6 *g* average acceleration. The load wall was instrumented with tri-axial load cells: three for the leg plate, two for the pelvis plate, two for the center console plate, and two for the thorax or abdomen plates, if used. Seat belt force transducers were used and sled acceleration was recorded. A nine-camera, 1000 f/s motion tracking system (Vicon Motion Systems, Centennial, CO) was used to quantify occupant kinematics in three dimensions (3D). Reflective targets were placed on the head, at T1, T12, and pelvis. Multiple targets on the head were digitized with respect to anatomical landmarks which facilitated measurements with respect to head center of gravity (CG). Reference targets were fixed to the sled and buck. Thus, head excursion measures are head CG movement with respect to the seat buck reference frame. All coordinate systems followed the SAE-j211 (version DEC 2003) standard sign convention.

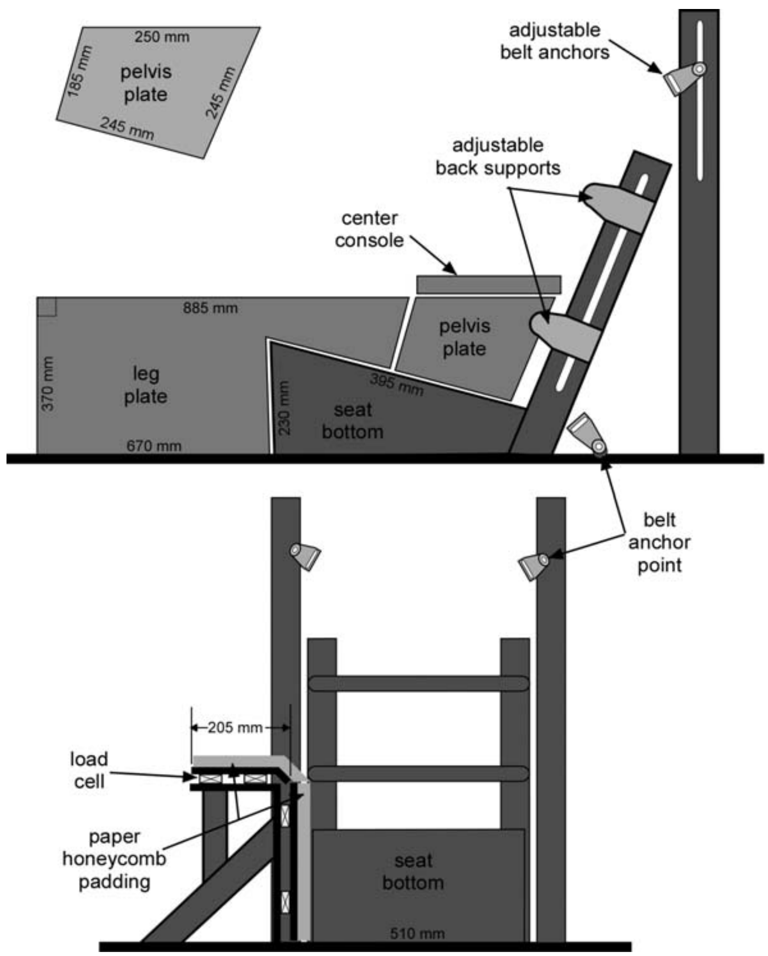

Figure 1. Schematic diagram, with dimensions, of far side sled buck viewed from the side (top) and from the front (bottom). The seat bottom angle with respect to horizontal was 15 degrees. Optional thorax or shoulder plates (100 mm X 460 mm not shown) were adjustable up/down/in/out.

Table 1. Test configurations and test identifiers

Config ID	Delta-V	Impact Angle	Plate	Shoulder belt	Belt Configuration	PMHS test (PMHS No.)	WorldSID test	THOR test
1	High	90	None	outboard	Mid, tension	HS104 (1)	WS119	TH155
2	Low	60	None	outboard	Mid	HS105 (2)	WS129	TH170
3	High	60	None	outboard	Mid	HS106 (2)	WS130	TH171
4	Low	90	Shoulder	inboard	Low	HS134 (3)	WS107	TH149
5	High	90	Shoulder	inboard	Low	HS135 (3)	WS108	TH150
6	Low	90	Thorax	inboard	Low	HS136 (3)	WS110	TH152
7	High	90	Thorax	inboard	Low	HS137 (3)	WS113	TH180
8	Low	90	None	inboard	High	HS140 (4)	WS115	TH156
9	High	90	None	inboard	High	HS141 (4)	WS118	TH177
10	Low	90	None	outboard	D-ring forward	HS138 (4)	WS132	TH174
11	High	90	None	outboard	D-ring forward	HS139 (4)	WS133	TH175
14	Low	60	None	inboard	High	HS166 (6)	WS124	TH168
15	High	60	None	inboard	High	HS167 (6)	WS126	TH169
16	High	90	Shoulder	outboard	Mid, tension	HS161 (5)	WS109	TH178
18	High	90	None	inboard	Low, tension	HS162 (5)	WS121	TH158
20	Low	60	None	outboard	Mid, tension	HS164 (6)	---	TH172
21	High	60	None	outboard	Mid, tension	HS165 (6)	---	TH173
22	High	90	None	outboard	Mid	HS163 (5)	---	TH176

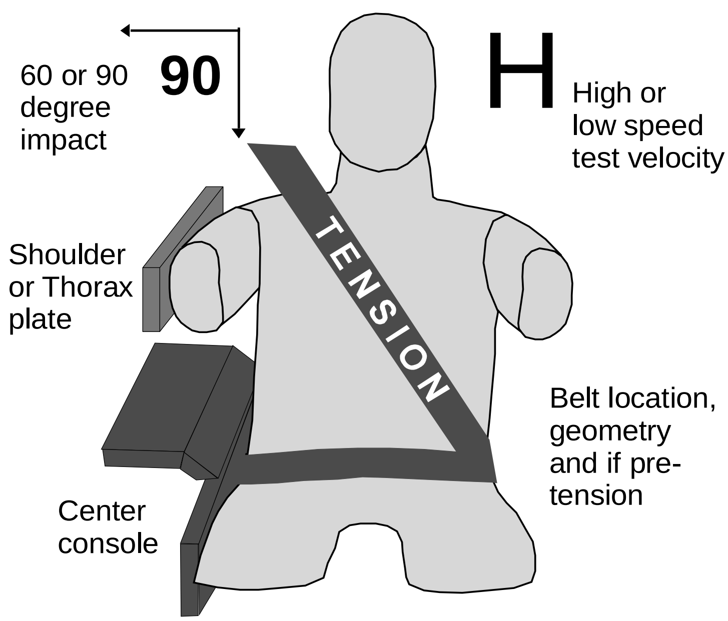

Figure 2. Explanation of figurines used as a visual code to clarify configurations depicted in tables and figures.

The series of 18 tests were conducted with six PMHS (Table 2). All studies with post mortem human subjects were reviewed and approved by the Institutional Review Board of the Milwaukee VA Medical Center Research Service. The PMHS were instrumented with triaxial accelerometer arrays at T1, T12, and sacrum. A custom-designed pyramid nine accelerometer package (PNAP) was used to derive head linear and angular accelerations [Yoganandan et al. 2006]. Using inverse dynamics formulae, the PNAP was also used to derive occipital condyle (OC) forces and moments [Pintar et al. 2005].

Table 2. PMHS specifications and tests.

Config ID	PMHS Test	PMHS	Age	Sex	Height (m)	Weight (kg)
1	HS104	1	80	M	1.73	67
2	HS105	2	81	M	1.75	70
3	HS106					
4	HS134	3	59	M	1.77	58
5	HS135					
6	HS136					
7	HS137					
10	HS138	4	74	F	1.55	70
11	HS139					
8	HS140					
9	HS141					
16	HS161	5	74	M	1.83	65
18	HS162					
22	HS163					
20	HS164	6	65	M	1.85	81
21	HS165					
14	HS166					
15	HS167					

A single 59-channel chestband (Denton, Inc. Rochester Hills, MI) was used at an appropriate location on the chest depending on the test configuration. For example, for a test with a thorax plate the chestband was placed around the level of the rib cage immediately adjacent to the plate; for an inboard belt test the chestband was placed lower on the rib cage to assess belt-induced deformations. Chest deflections were recorded in all PMHS tests except for configurations where a shoulder plate was used or in the 90-degree test where there was a “high” inboard shoulder belt orientation. Chest deflections for PMHS tests were taken at the point along the chestband that yielded the maximum value. For each PMHS run, placement in the seating buck consisted of arms outstretched (driving position), head Frankfort plane horizontal, and right hip just touching the pelvis center console plate. Immediately post-test, PMHS were palpated for bony fractures. After all tests were conducted, a complete x-ray examination and an autopsy identified injuries. The head was isolated and measured for center of gravity (CG) and moment of inertia (MOI). The head of the PMHS was isolated by dissecting the skin along the inferior mandible, continuing through the occipital condyles, and through the skin along a line just inferior to the posterior base of the skull. The head CG was obtained by suspending the head from a cable along multiple points in the mid-sagittal plane and obtaining the intersection of plumb lines. The MOI about the primary anatomical axes was obtained using a standard three-cord torsional pendulum.

For each test that was conducted with a PMHS, duplicate ATD tests were also conducted (Figure 3). Except for the last three configurations (Configurations 20-22), a 50th percentile WorldSID production model was used in one ATD series (Table 1). The placement of the WorldSID in the seat buck mimicked the PMHS seating position with the half arms in the horizontal position and the pelvis touching the pelvis plate. The WorldSID instrumentation included head linear and angular accelerations, upper/lower neck loads, chest deflections (IR-TRACC), T1, T12 spine accelera-tions, and pelvic accelerations.

A THOR (NT model, Gesac, Inc) was used in another ATD test series. Its arms, like the PMHS, were in the driving position attached loosely to a bar that simulated the location of the steering wheel. The THOR pelvis was positioned in the seat just touching the load wall. The THOR was modified by the manufacturer for side impact use by inserting additional foam padding over the lateral rib cage and moving the upper-right CRUX-pot to the direct-lateral position. Besides the CRUX-pots, similar instrumentation was used with head linear and angular accelerometers, spine and pelvis accelerometers and upper neck load cell.

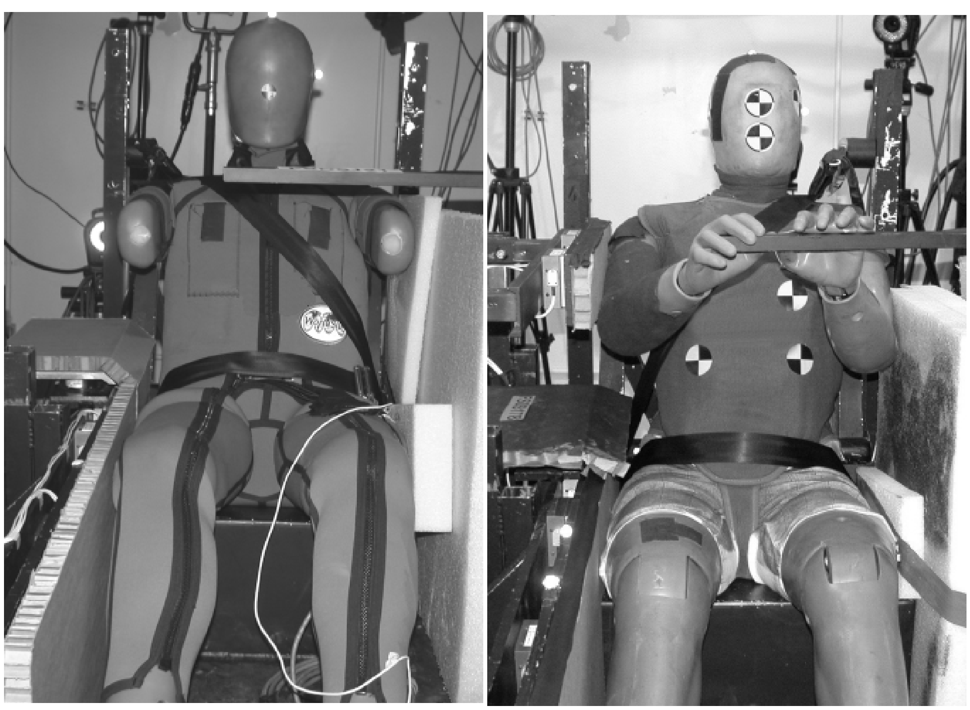

Figure 3. Pre-test photos of WorldSID (left) with inboard belt in low position (Config-18) and THOR-NT (right) with outboard belt and shoulder plate (Config-16).

3 RESULTS

Each PMHS test was compared to the corresponding dummy test by over-plotting the resulting responses (Appendix). Minimum and/or maximum values of responses were obtained for comparison (Tables 3-4).

In general, low speed tests (Configurations 2, 4, 6, 8, 10, 14, 20) produced much lower magnitude responses compared to equivalent high speed test configurations (Table 3). Low speed tests were conducted to evaluate dummy biofidelity at lower delta-v and to ensure that all measurement systems were functioning together. Maximum head CG linear accelerations for low speed PMHS tests were 3-9 *g*, and 1-18 *g* for dummy tests. Maximum T1 and T12 spine accelerations were 3-16 *g* for PMHS low speed tests and 5-15 *g* for dummy low speed tests. Low speed test shoulder belt maximum loads were 42-996 N and lap belt loads were 40-656 N.

From examining high speed video and deformed PMHS chest contour shapes, it was determined that the shoulder belt was responsible for the maximum chest deflection for configurations 1, 2, 3, 10, 11, 20, 21, 22; the center console was responsible for maximum chest deflections for configurations 14 and 15; the thorax plate induced maximum deflections for configurations 6 and 7.

Maximum Y-direction head CG excursions were examined as a function of restraint for high speed 90-degree tests (Figure 4). The shoulder belt outboard with a forward D-ring position (Configuration 11) generally produced the most lateral head excursion. When the D-ring position was lowered and more rearward (Configuration 22) or when the belt system had pre-tension (Configuration 1), there was only a slight decrease in lateral head excursion. Only when there was a restraining plate (Configurations 5, 7, 16) were the head excursions appreciably reduced. There were not as many 60-degree tests to make the same comparisons but the same general trend was apparent for the three high speed tests (Configurations 3, 15, 21). The head CG excursion plots in three planes are given in the appendix. The starting point for each dummy head excursion in the Y-direction was normalized to the initial location of the PMHS head (at approximately 300 mm from the seat left corner reference point). The difference in the starting point for the dummies with respect to the X- and Z-directions was not normalized with respect to PMHS. In other words, the offsets in the plots are representative of how each dummy sits in the seat in its initial location. In general, the WorldSID head begins in a more forward position than the THOR head. The PMHS head starting position varied depending on individual anthropometry. From these plots, it can also be appreciated that the WorldSID follows the PMHS head excursion well for 90-degree tests, and the THOR follows the PMHS head excursions well for the 60-degree tests.

The loads derived for the occipital condyles (OC), Fx, Fz, and Mx, (Appendix) were not always of the same magnitude between dummy and PMHS, but almost always followed the same curve morphology. The exception to this was when the inboard belt was placed in the “high” position (Configurations 8, 9, 14, 15) over the neck to evaluate worst-case belt loading. The lateral shear load especially was often of opposite sign between PMHS and either dummy.

Comparing load wall responses between dummies and PMHS, there was often the same response pattern and timing (Appendix). WorldSID maximum load wall forces however, were always greater than PMHS and often significantly (more than 500 N) greater. THOR pelvic forces were sometimes greater and sometimes less than PMHS. When a thorax plate was in place (Configuration 6, 7) both dummies reproduced PMHS response fairly well. With a shoulder plate (Configurations 4, 5, 16) however, the THOR produced significantly higher shoulder plate loads than PMHS or WorldSID.

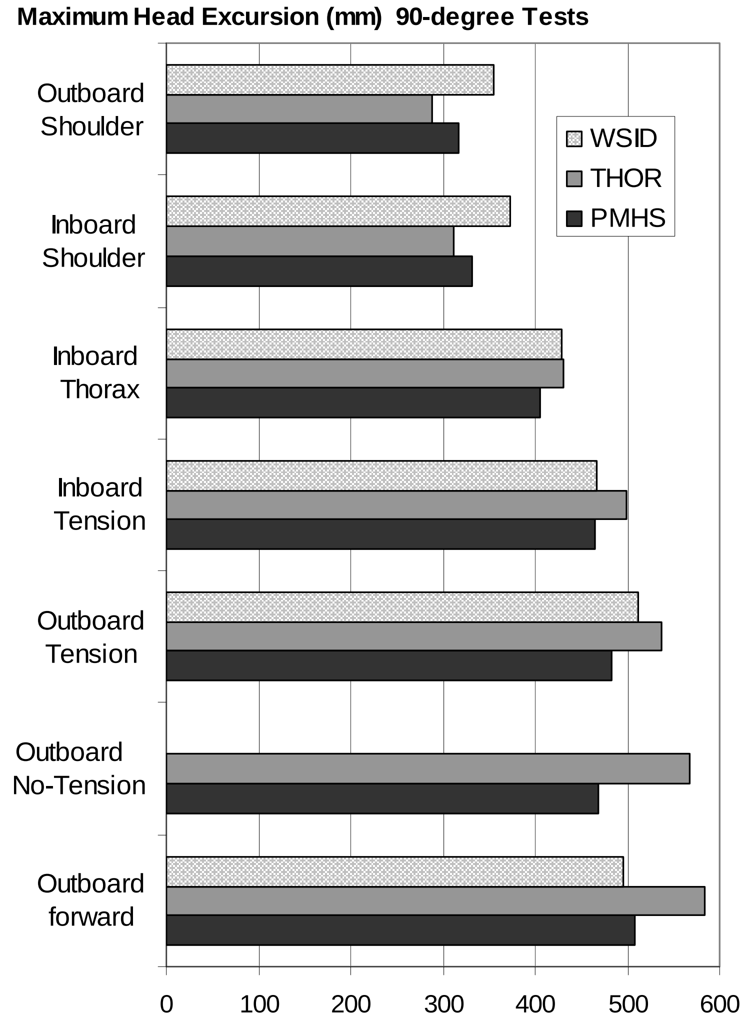

Figure 4. Bar graph representation of maximum head excursions in the Y-direction as a function of restraint.

Table 3. Maximum values from transducer data and calculated responses.

Config ID	Test Code	OCC FZ (N)	OCC FY (N)	OCC MX (Nm)	Y head excursion (mm)	Shoulder Belt Load (N)	Lap Belt Load (N)	Pelvic Load Y (N)	Thorax / Shoulder Load Y(N)	Chest Deflection (mm)
1	HS104	1012	-744	-57	483	2950	855	-4162	---	62
	WS119	1467	-648	-42	512	2800	894	-5055	---	23 (A2)
	TH155	1702	-760	-97	537	2935	998	-4863	---	45 (LR)
2	HS105	169	-184	-11	394	784	336	-1755	---	24
	WS129	228	-295	-22	300	996	343	-2418	---	7 (A1)
	TH170	291	-209	-15	330	895	368	-1981	---	9 (LR)
3	HS106	1314	-797	-53	536	3817	997	-3771	---	49
	WS130	1182	-560	-36	428	3014	1172	-4380	---	15 (T3)
	TH171	1280	-458	-61	489	3575	1302	-3425	---	37 (LR)
4	HS134	233	-181	-31	164	78	107	-1846	-1958	---
	WS107	205	-228	-18	198	42	49	-2860	-1894	22 (s)
	TH149	305	-340	-30	166	86	83	-1880	-3030	7 (UL)
5	HS135	1085	-1500	-126	332	464	513	-3218	-3827	---
	WS108	888	-451	-64	373	326	261	-4884	-3227	43 (s)
	TH150	971	-595	-60	312	341	220	-3267	-6876	20 (UL)
6	HS136	208	-174	-17	217	160	160	-1688	-2093	46
	WS110	210	-241	-24	203	168	266	-2044	-2511	32 (T2)
	TH152	197	-266	-19	195	89	102	-2040	-2021	17 (UR)
7	HS137	1412	-804	-61	406	795	710	-4115	-3851	68
	WS113	805	-497	-43	428	1235	603	-4247	-3491	64 (T2)
	TH180	1344	-498	-87	430	1300	855	-3925	-4228	39 (UR)
8	HS140	103	-127*	-8	269	188	92	-1340	---	---
	WS115	314	-343	-29	330	541	372	-2951	---	12 (A2)
	TH156	252	-145	-28	284	687	329	-2361	---	15 (UL)
9	HS141	1639*	-1167*	-41	465	2093	539	-3733	---	---
	WS118	1795	-945	-57	463	2795	1849	-5663	---	28 (A2)
	TH177	334	-159	-37	378	3370	2348	-3970	---	40 (UL)
10	HS138	138	-169	-12	301	757	237	-1779	---	31
	WS132	306	-386	-28	351	610	317	-3143	---	12 (A2)
	TH174	306	-357	-27	373	852	299	-2193	---	9 (LR)
11	HS139	1175	-661	-48	509	2406	622	-4380	---	48
	WS133	1149	-606	-42	496	1693	715	-5007	---	20 (T3)
	TH175	1537	-642	-77	583	3566	865	-4677	---	58 (LR)
14	HS166	306*	-176	-11	369	786	662	-1885	---	69
	WS124	278	-259	-22	269	764	469	-2387	---	7 (A2)
	TH168	188	-130	-18	272	809	333	-1534	---	13 (UL)
15	HS167	897	-860	-32	440	2939	1842	-4000	---	83
	WS126	1420	-673	-39	357	2746	1846	-4089	---	20 (A2)
	TH169	689	-528	-45	378	4057	2578	-2443	---	34 (UL)
16	HS161	1502*	-900*	-59	317	1123	298	-3044	-3219	---
	WS109	1048	-354	-84	355	695	372*	-4637	-2844	30 (S)
	TH178	1107	-531	-58	288	597	268	-3447	-5842	13 (UL)
18	HS162	2165*	-1845*	-47	465	1351	1010	-2956	---	---
	WS121	1959	-842	-53	466	2244	1515	-5041	---	27 (A2)
	TH158	1139	-508	-108	499	3588	1883	-5579	---	31 (UL)
20	HS164	105	-105	-6	420	716	516	-1943	---	40
	---	---	---	---	---	---	---	---	---	---
	TH172	163	-208	-15	321	865	356	-1814	---	9 (UL)
21	HS165	861	-480	-29	538	3507	1142	-4586	---	84
	---	---	---	---	---	---	---	---	---	---
	TH173	1159	-584	-58	484	3348	1400	-3455	---	34 (LR)
22	HS163	1980*	-995	-37	469	2236	497	-3593	---	80
	---	---	---	---	---	---	---	---	---	---
	TH176	1652	-634	-96	568	3212	835	-4394	---	44 (LR)

* Denotes peak value located at spike in data set.
S, A1, A2, T1, T2, T3 denote peak value recorded from WorldSID shoulder abdomen or thorax rib 1, 2, 3.
UL, UR, LR denotes peak value recorded from THOR crux upper left, upper right, or lower right

Table 4 Maximum/minimum values from transducers and calculated data.

Config ID	Test Code	Head CG Linear Accel. YL (G'S)	Head CG Linear Accel. ZL (G'S)	Head Angular Acceleration XL-Max (Rad/s/s)	Head Angular Acceleration XL-Min (Rad/s/s)	Head Angular Acceleration ZL-Max (Rad/s/s)	Head Angular Acceleration ZL-Min (Rad/s/s)	T1 Accel. YL (G'S)	T12 Accel. YL (G'S)	Sacrum/Pelvis Accel. YL (G'S)
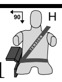 1	HS104	-22	31	1982	-1803	345	-1157	-25	-16	-22
	WS119	-15	35	2425	-2740	685	-779	-21	-18	-19
	TH155	-35	13	327	-4591	1921	-2122	-18	-16	-19
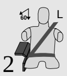 2	HS105	-6	4	459	-462	177	-180	-8	-8	-12
	WS129	-7	6	1164	-789	177	-147	-8	-8	-11
	TH170	-5	6	436	-324	295	-457	-6	-9	-11
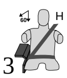 3	HS106	-21	35	2416	-1680	1264	-1393	-37	-19	-18
	WS130	-14	29	2074	-1966	578	-490	-14	-16	-18
	TH171	-24	32	2204	-2472	1342	-3991	-16	-23	-31
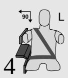 4	HS134	-4	6	1001	-1078	351	-425	-12	-16	-12
	WS107	-6	5	712	-422	233	-191	-10	-12	-13
	TH149	-8	8	779	-774	225	-195	-15	-11	-11
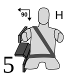 5	HS135	-36	26	2364	-2042	1157	-1608	-42	-24	-19
	WS108	-36	19	2137	-3992	963	-2454	-21	-25	-20
	TH150	-25	24	2524	-1552	532	-816	-68	-21	-16
 6	HS136	-5	5	775	-542	310	-264	-11	-15	-11
	WS110	-7	5	762	-1213	305	-568	-11	-10	-15
	TH152	-6	5	408	-457	141	-231	-10	-12	-11
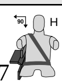 7	HS137	-19	34	2458	-1129	1189	-616	-34	-40	-21
	WS113	-13	20	963	-1677	362	-424	-17	-17	-19
	TH180	-30	32	1058	-1995	897	-2718	-18	-19	-20
 8	HS140	-4	3	472	-407	282	-419	-6	-10	-10
	WS115	-9	7	1270	-1151	393	-725	-8	-11	-13
	TH156	-8	1	355	-519	746	-656	-7	-10	-13
 9	HS141	-32	46	3902	-6087	1914	-1019	-23	-21	-22
	WS118	-19	43	2994	-2939	843	-808	-29	-15	-20
	TH177	-40	9	1364	-2222	5157	-2676	-29	-16	-20
 10	HS138	-5	4	474	-318	191	-125	-5	-9	-10
	WS132	-10	7	1379	-1600	342	-269	-9	-8	-13
	TH174	-8	7	413	-520	177	-202	-6	-9	-11
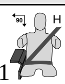 11	HS139	-18	44	5151	-5102	4334	-6003	-16	-24	-24
	WS133	-13	28	2013	-2185	708	-512	-15	-118	-18
	TH175	-25	36	1087	-2273	1116	-2906	-16	-17	-23
 14	HS166	-7	9	506	-394	442	-478	-4	-7	-9
	WS124	-7	7	1384	-707	384	-259	-9	-9	-12
	TH168	-18	6	1736	-952	3503	-1521	-5	-9	-11
 15	HS167	-23	24	1619	-1325	1209	-2428	-23	-16	-19
	WS126	-16	34	2524	-1769	634	-804	-22	-13	-19
	TH169	-14	22	1534	-690	1761	-1632	-25	-19	-26
 16	HS161	-25	41	2646	-4185	1928	-2616	-44	-25	-19
	WS109	-33	26	5081	-4593	1130	-2219	-19	-22	-20
	TH178	-24	22	2229	-1498	623	-1507	-72	-22	-19
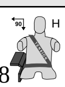 18	HS162	-51	69	4344	-4977	2927	-1987	-79	-20	-18
	WS121	-22	46	2739	-3674	816	-884	-28	-68	-20
	TH158	-27	11	1418	-4071	1719	-4408	-27	-18	-26
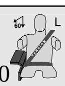 20	HS164	-3	3	230	-202	282	-283	-3	-7	-9
	---	---	---	---	---	---	---	---	---	---
	TH172	-5	5	400	-290	232	-188	-6	-9	-11
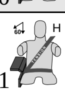 21	HS165	-13	23	1380	-909	838	-1684	-13	-16	-15
	---	---	---	---	---	---	---	---	---	---
	TH173	-23	30	2547	-2304	1267	-4406	-15	-20	-23
 22	HS163	-30	57	3089	-3262	1246	-2144	-19	-18	-18
	---	---	---	---	---	---	---	---	---	---
	TH176	-32	38	963	-3822	1362	-3494	-18	-19	-25

Note: XL, YL, ZL denote values are given in local anatomical reference frame.

Injuries sustained by each PMHS are provided in Table 5. For the first three PMHS the major injury was rib fracture. For the first and second PMHS the rib fractures were caused by shoulder belt loading seen as direct compression to the lower right rib cage. The third PMHS experienced shoulder plate loading in the first two configurations, and thorax plate loading in the last two configurations. The rib fractures were in the vicinity of where the thorax plate loaded the rib cage. The fourth PMHS experienced a 'worst-case' outboard belt config-uration where the anchor point was forward of the mid, or 'normal,' position. This caused the shoulder of the PMHS to slip out of the belt and resulted in maximal head excursion. There were only two rib fractures in this PMHS. There was however, a fairly serious T4-T5 separation which was unstable enough to imply some type of cord contusion. This PMHS also experienced a 'worst-case' inboard belt loading condition where the shoulder belt anchor point was placed high across the mid portion of the neck on the right side. This configuration resulted in abrasions and even contusions in the subcutaneous fat seen upon dissection of the area. The belt location is likely responsible for the intimal tear in the left carotid artery on the opposite side of belt loading due to stretching of the carotid artery.

The fifth PMHS experienced three high-speed tests which resulted in several injuries. The first of these three tests was with a shoulder plate and an outboard belt; the shoulder belt load was the lowest (1123 N) of the three tests. The shoulder plate likely caused the shoulder dislocation and fracture, as well as the clavicle and scapula fractures. The inboard belt configuration produced moderate belt loads (1351 N); the outboard belt configuration produced higher belt loads (2236 N). It was noted from the high speed video that the belt did not slip off the shoulder for this last test (Configuration 22). There were spleen, liver, and a significant stomach laceration; it is unknown which of the three tests produced each of these internal injuries. After the second of the three test runs, it was noted that palpable rib fractures were present on the right side. The chestband data for test HS163 showed 80 mm of displacement to the right lateral rib cage. For the sixth PMHS, again, right sided rib fractures were present with two left rib fractures. This PMHS experienced all 60-degree tests. The outboard belt produced 84 mm of deformation and the interaction with the center console on the inboard belt test produced 83 mm of chest compression. The fracture-separation of the right acromioclavicular joint was probably due to arm fling.

Table 5: PMHS Injuries

PMHS	Testing Sequence	Injury Description	AIS
1	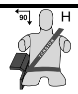	1 left rib fx: rib 7; 5 right rib fxs: ribs 3, 7-9	3
		C7 fracture from degeneration	2
2	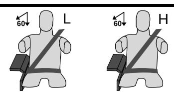	6 right rib fxs: ribs 3-8	3
3	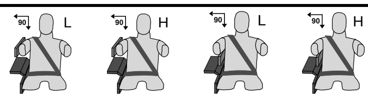	5 right rib fxs: ribs 4, 7-9	3
4	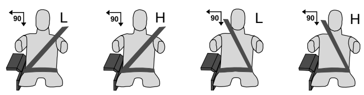	Abrasion, contusion right side of neck	1
		Left external carotid artery intimal tear	2
		2 left rib fxs on rib 3	2
		T4-T5 separation with T4 fx; possible cord contusion	3
5	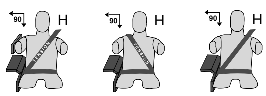	Multiple rib fxs: right 1-10, left 1-7; with pneumothorax and flail chest	5
		Liver laceration	2
		Spleen laceration	2
		Stomach laceration	3
		Right Clavicle fracture through acromio-clavicular joint	2
		Right Scapula fracture	2
		Right shoulder dislocation and fracture through glenoid	2
6	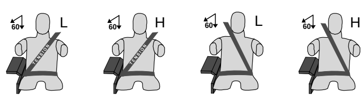	5 right rib fxs: ribs 3-7; 2 left rib fxs: ribs 5-6	3
		Sternum fracture at rib 4	2
		Fracture/separation right acromio-clavicular joint	2
		Left humerus head fracture	2

4 DISCUSSION

Despite contributing to a significant portion of the injuries and Harm [Malliaris et al. 1982] in vehicle crashes far side impacts have received little attention in the literature. It has been noted that because many of the counter-measures that may be effective for reducing head injuries in far side crashes (e.g., inflatable curtains) may also be effective for roll-over crashes, safety systems could have greater protection capability [Digges and Gabler 2006]. The ability to assess vehicle crashworthiness for far side occupants however, depends on the biofidelity of the dummy in the far side loading condition. Since there is currently no dummy that is designed specifically for far side collisions, the primary goal in the current series of tests was to perform a preliminary investigation of the biofidelity of THOR and WorldSID in far side impacts. A secondary goal was to evaluate the efficacy and trade-offs of generic countermeasures.

A sled buck was designed to specifically evaluate the far side impact event in a controlled laboratory environment. This buck was designed with moveable plates and adjustable restraint systems so that PMHS of different sizes would load the generic restraint systems in the same manner as the dummies. For example, a shoulder plate could be moved to optimally load the shoulder of any sized PMHS in the same manner as it would in a 50th percentile sized dummy, and a seat belt anchor point could be aligned with respect to subject anthropometry. This facilitated direct dummy biofidelity evaluation because restraint systems loaded the same location on the body for PMHS and dummy. The buck consisted of a rigid seat design with easy-to-obtain paper honeycomb where padding was needed. The two adjustable rigid cylinders provided back support and maintained visualization for body target movements in three dimensions. The center console remained in place for all tests as this was considered a standard configuration in late-model vehicles. The seat belt anchor points could be moved such that locations could be made with respect to body landmarks (e.g., horizontal to top of shoulder). All of these adjustments were built-in to ensure robustness in biofidelity evaluations.

Previous epidemiological studies implicated the far side interior as a causative agent for head injuries [Gabler et al. 2005]. One of the main purposes therefore, of the generic countermeasures was to reduce head excursion in the direction of the crash vector. This was accomplished in the generic countermeasures using belt system geometry and placement, as well as thorax or shoulder support in the form of padded plates. It was observed in the thorax plate countermeasure that rib fractures resulted from plate loading. A similar observation was noted by Melvin and Gideon (2004) in the design of racing vehicles for side impact protection that a “rib protector” was less desirable than shoulder protection. This is not to imply that a “thorax-type” countermeasure, could not work in the real vehicle environment. An example of the implementation of a thorax or shoulder support for far side impacts has been proposed using an airbag system [Bostrom and Haland, 2003]. Because the WorldSID response in the thorax plate test in the current study mimicked PMHS response well, this dummy could be used to evaluate such types of countermeasure designs.

Existing outboard belt restraint systems may have a D-ring position that allows the torso of the occupant to slip out of the shoulder belt in a far side impact collision. In a previous examination of real-world crashes Mackay et al. (1991) estimated that the torso slipped out of the shoulder belt approximately 35% of the time. Recent real-world data for restrained occupants in far side crashes indicate that 27% of the AIS=3+ injuries occur to the head [Gabler et al. 2005]. When AIS=3+ injuries and all fatalities are considered, 42% of the Harm for belted occupants occurs to the head [Digges et al. 2005]. Results of the present test series indicated head excursions can still be greater than 400 mm even when the occupant does not slip out of the belt. The addition of pre-tension and belt placement directly over the shoulder reduced head excursion by about 50 mm. Only when shoulder or thorax restraining plates were used, did head excursion reduce by more than 150 mm compared to the condition where belt slip occurred. These data indicate that even without slipping out of the belt the head can still move quite extensively within the vehicle during a far side crash.

Countermeasures that reduce head excursions must be designed to not increase the likelihood of injury to other body regions. The thorax restraint used in the present study increased lateral chest displacements to injurious levels. An inboard shoulder belt also reduced head excursions, but proper belt placement is critical. Specific placement directly over the shoulder is easier to control in a dummy than it would be in a real human. A mispositioned shoulder belt, such as the high position for the inboard belt (Configurations 8-9, 14-15) may cause high loads and neck lateral bending, placing the internal structures such as the vascular system and spinal column at risk for trauma

[Sinson et al. 2003]. Rouhana et al. (2006) tested a four-point belt system using PMHS in a far side impact mode and demonstrated no carotid artery injury with optimal “low” belt positioning. In the PMHS test for configuration-9 with a “high” belt position a carotid artery intimal tear was found after histological sectioning was done. This injury did not occur on the “pinching” (right) side, but rather on the “stretching” (left) side. The tension mechanism for carotid artery intimal tears has been well documented [Stemper et al. 2007] and appears to be the cause in this case. The PMHS test instrumentation did not allow for deriving lower neck loads in the present test series, but the WorldSID lower neck lateral shear load (Fy) reported previously [Pintar et al. 2006] demonstrated greater magnitudes and opposite sign compared to tests with optimal belt positions. This lower neck lateral shear load in dummy tests may be a good indicator of sub-optimal belt positioning when using inboard belts.

Two advanced dummies were evaluated for biofidelity in the current test series: the THOR-NT and the WorldSID. The WorldSID production version dummy provides extensive instrumentation to evaluate near side impacts. The WorldSID dummy used in the present test series was not modified in any way except to move the chest deflection sensors to the right side when they are usually placed on the left. It has a self-contained data acquisition system that allows for complete internal wiring of accelerometers, load cells, and deflection sensors. The WorldSID has direct lateral shoulder deflection measurement capability and mimicked the PMHS shoulder responses well. This is advantageous for shoulder-type countermeasure design. The WorldSID has a unique design of the lumbar spine that looks like an inverted “U” which allows for lateral motion of the torso relative to the pelvis. This lateral torso motion has been shown to be unique in PMHS testing and may be the reason the head can contact the opposite side door in far side crashes [Fildes et al. 2002]. There are some limitations of this dummy for use in far side impact crashes, a mode that it was not originally designed for. Each of the ribs has an internally mounted IR-TRACC [Rouhana et al. 1998] that measures deflection best when impacted in a purely lateral direction. These sensor locations worked well when the plate-type countermeasures were included in the test configuration. With belt-like countermeasures these locations were sub-optimal. The interaction of the outboard shoulder belt with the oblique portion of the right lower rib cage demonstrated in the PMHS test was not fully recorded by the laterally-placed IR-TRACC sensors. Thus belt-like countermeasure tests evaluated by the WorldSID would require relocation of existing sensors or use of other types of sensors. Given the design of the WorldSID chest and rib cage, relocation of sensors should be possible.

The THOR-NT was initially designed as a frontal impact dummy. With some modifications, the manu-facturer does also recommend it for use in limited side impact applications. The THOR-NT used for the current test series had extra foam padding over the lateral rib cage and the right antero-lateral CRUX pot was moved to a direct lateral position. The THOR-NT has an articulated spine which appeared to aid more biofidelic lateral torso movement. During outboard belt loading cases the CRUX pot system of the THOR in the lower right rib cage sensed a majority of the maximum deformation caused by the shoulder belt in this area. Given the complex nature of the belt loading in the far side impact environment however, the THOR lower right CRUX pot is still not optimally placed for all configurations. In general the THOR-NT responded with biofidelic chest loads when the belt was the primary restraint, and was particularly better in the 60-degree orientation tests. It was not as good at reproducing human-like shoulder response when a plate-type restraint was present. Again, the design of the THOR-NT shoulder was not intended for direct lateral impact.

Limitations of this study include a limited test series. Six PMHS were used to conduct eighteen tests. In general, low velocity tests (11 km/h) were designed such that no injuries would occur. This was readily apparent given that all tests were conducted with some type of belt restraint and the maximum values recorded by sensors were at sub-injurious levels. For the PMHS that experienced more than one high speed impact, the configurations were designed to produce distinct injury patterns. For example, test HS135 was a shoulder-plate restraint and produced no shoulder injuries, and test HS137 was a thorax-plate restraint and produced some rib fractures adjacent to the plate. Also, test HS139 was an outboard belt test where the PMHS slipped out of the belt and the second high speed test that this PMHS experienced was a mis-positioned inboard belt test. The PMHS experienced a serious thoracic spine injury, which can be assumed to be due to the outboard belt test, and a carotid artery tear, which can be assumed to be due to the inboard belt test. The exception to this pattern was PMHS-5 wherein three high speed tests were conducted. The extensive and multiple injuries this PMHS experienced are difficult to assign to particular test configurations. The resulting response curves including head excursion and chest deflection however, do not demonstrate a pattern indicative of increasing extent of injury, and therefore the responses for biofidelity evaluation should be adequate.

Another limitation is that the biofidelity assessments are based upon a single PMHS response test. To conduct a more complete biofidelity evaluation multiple tests should be conducted at each configuration and response corridors should be derived as has been done in previous studies [Hardy et al. 2001; Maltese et al. 2002; Kent et al. 2004]. The decision early in the planning stages of this project was to conduct single tests with many configurations rather than to conduct multiple repeated tests under a small number of configurations. Since the main objective was to compare responses between PMHS and current dummies with and without generic countermeasures, the greater number of configurations was deemed to be ultimately more helpful to cover the potential realm of future countermeasure design.

5 CONCLUSION

PMHS testing in the far side impact crash mode demonstrated inboard shoulder belts that were positioned directly over the shoulder, as well as countermeasures that promoted alternate load paths such as shoulder or thorax restraints, reduced head excursion and helped contain the occupant. The specific design characteristics of these counter-measures must be such that local chest deflections are not injurious. Both the WorldSID and THOR-NT response in far side impact compared favorably to PMHS response, considering that these dummies were not designed for this crash mode. The WorldSID performed better in plate-like countermeasure tests and in general, for 90-degree tests. The THOR-NT performed better in belt-like countermeasure tests and in general, for 60-degree tests. Although both dummies appear to have biofidelic rib cages, the individual location of chest deflection measurement may not be optimal. The far side impact environment is complex with multiple potential sources of injury to the human occupant. The THOR and the WorldSID dummies demonstrate adequate biofidelity to develop countermeasures in this crash mode and would be enhanced by specific instrumentation changes to detect trade-offs in countermeasure design.

6 REFERENCES

Augenstein J, Perdeck E, Martin P, Bowen J, Stratton T, Horton T, Singer M, Digges K, Steps J. (2000) Injuries to restrained occupants in far-side crashes. 44th Annual Proceedings, Association for the Advancement of Automotive Medicine, Barrington, IL pp 57-66.

Banglmaier RF, Rouhana SW, Beillas P, Yang KH. (2003) Lower extremity injuries in lateral impact: A retrospective study. 47th Annual Proceedings, Association for the Advancement of Automotive Medicine, Barrington, IL pp 425-444.

Bostrom O, Haland Y. (2003) Benefits of a 3+2 point belt system and an inboard torso side support in frontal, far-side, and rollover crashes. 18th ESV conference proceedings, Nagoya, Japan.

Digges KH, Gabler HC, Mohan P, Alonso B. (2005) Characteristics of the injury environment in far-side crashes. 49th Annual Proceedings, Association for the Advancement of Automotive Medicine, Barrington, IL pp 185-197.

Digges KH, Gabler HC. (2006) Opportunities for reducing casualties in far-side crashes. SAE World Congress Meeting (2006-01-0450), Warrendale, PA, SP-1997.

Fildes BN, Sparke LJ, Bostrom O, Pintar FA, Yoganandan N, Morris AP. (2002) Suitability of current side-impact test dummies in far-side impacts. Proceedings IRCOBI, 19th International Conference on the Biomechanics of Impact, Lyon, France pp 43-56.

Frampton RJ, Brown R, Thomas P, Fay P. (1998) The Importance of non struck side occupants in side collisions. 42nd Annual Proceedings, Association for the Advancement of Automotive Medicine, Barrington, IL pp 303-320.

Franklyn M, Fitzharris M, Yang K, Frampton R, Morris A, Fildes B. (2002) Aortic injuries in side impacts: A preliminary analysis. 46th Annual Proceedings, Association for the Advancement of Automotive Medicine, Barrington, IL pp 1-12.

Gabler HC, Digges K, Fildes BN, Sparke L. (2005) Side impact injury risk for belted far side passenger vehicle occupants. SAE World Congress, paper # 2005-01-0287, Society of Automotive Engineers, Warrendale, PA.

Haland Y, Lovsund P, Nygren A. (1990) Estimation of fatalities and disabilities in car-to-car side impacts: An evaluation of different risk factors. 34th Annual Proceedings, Association for the Advancement of Automotive Medicine, Barrington, IL pp 275-287.

Hardy WN, Schneider LW, Rouhana SW. (2001) Abdominal impact response to rigid-bar, seatbelt, and airbag loading. Stapp Car Crash Journal 45:1-31.

Kent R, Lessley D, Sherwood C. (2004) Thoracic response to dynamic, non-impact loading from a hub, distributed belt, diagonal belt, and double diagonal belts. Stapp Car Crash Journal 48: 495-519.

Mackay GM, Parkin S, Hill J, Munns JAR. (1991) Restrained occupants on the non-struck side in lateral collisions. 35th Annual Proceedings, Association for the Advancement of Automotive Medicine, Barrington, IL pp 119-132.

Malliaris AC, Hitchcock R, Hedlund J. (1982) A search for priorities in crash protection. SAE International paper #820242. Society of Automotive Engineers, Warrendale, PA.

Maltese MR, Eppinger RH, Rhule HH, Donnelly BR, Pintar FA, Yoganandan N. (2002) Response corridors of human surrogates in lateral impacts. Stapp Car Crash Journal 46:321-351.

Melvin JW, Gideon T. (2004) Biomechanical principles of racecar seat design for side impact protection. SAE International, paper #2004-01-3515. Society of Automotive Engineers. Warrendale, PA.

Pintar FA, Yoganandan N, Baisden J. (2005) Characterizing occipital condyle loads under high-speed head rotation. Stapp Car Crash Journal 49:33-47.

Pintar FA, Yoganandan N, Stemper BD, Bostrom O, Rouhana SW, Smith S, Sparke L, Fildes BN, Digges KH. (2006) WorldSID assessment of far side impact countermeasures. 50th Annual Proceedings, Association for the Advancement of Automotive Medicine, Barrington, IL pp 189-209.

Rouhana, SW, Elhagediab, AM., Chapp JJ. (1998) A high-speed sensor for measuring chest deflection in crash test dummies. Proceedings of 16th International Technical Conference on Enhanced Safety of Vehicles, Technical Paper No. 98-S9-O-15, Windsor, Canada.

Rouhana SW, Kankanala SV, Prasad P, Rupp JD, Jeffreys TA, Schneider LW. (2006) Biomechanics of 4-Point seat belt systems in farside impacts. Stapp Car Crash Journal, 50:267-298.

Sinson GP, Yoganandan N, Pintar FA, Morgan RM, Maiman DJ, Brasel KJ, Gennarelli TA. (2003 Carotid artery trauma in motor vehicle crashes: Investigation of the local tensile loading mechanism. Proceedings IRCOBI, 20th International Conference on the Biomechanics of Impact, Lyon, France pp 207-216.

Stemper BD, Yoganandan N, Pintar FA. (2007) Mechanics of arterial subfailure with increasing loading rate. Journal of Biomechanics 40(8):1806-1812.

Yoganandan N, Pintar FA, Gennarelli TA, Maltese MR. (2000) Patterns of abdominal injuries in frontal and side impacts. 44th Annual Proceedings, Association for the Advancement of Automotive Medicine, Barrington, IL pp 17-36.

Yoganandan N, Zhang J, Pintar FA, Liu YK. (2006) Lightweight low-profile nine-accelerometer package to obtain head angular accelerations in short-duration impacts. Journal of Biomechanics 39:1347-1354.

APPENDIX

Please see the following pages for plots comparing responses from PMHS, WorldSID, and THOR-NT tests. Each test configuration is shown schematically by a small figurine and response graphs are demonstrated. Results from testing have been provided in electronic form to the sponsors for appropriate dissemination.

Appendix

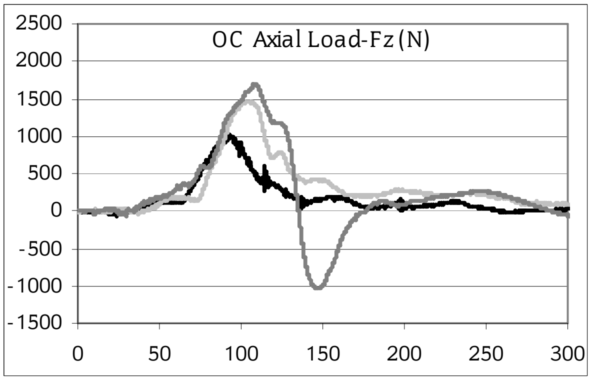

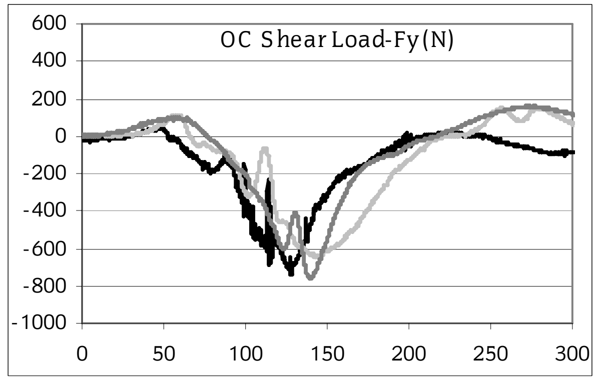

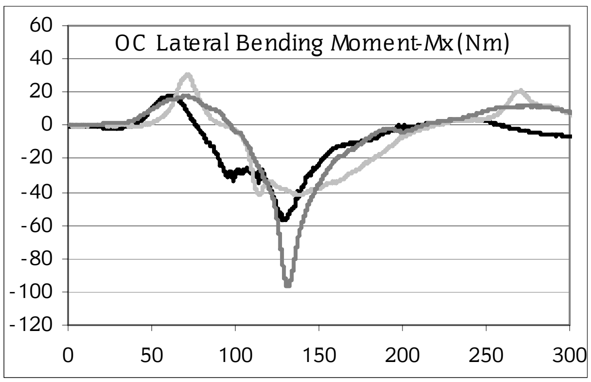

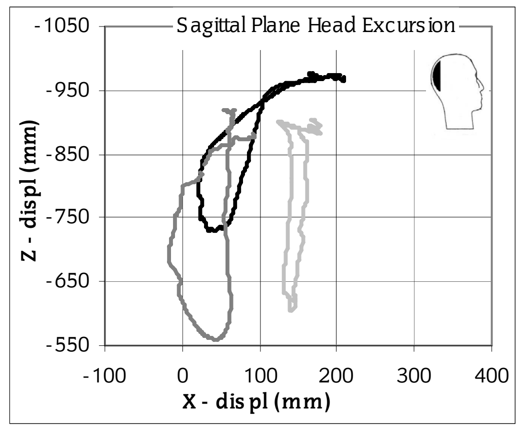

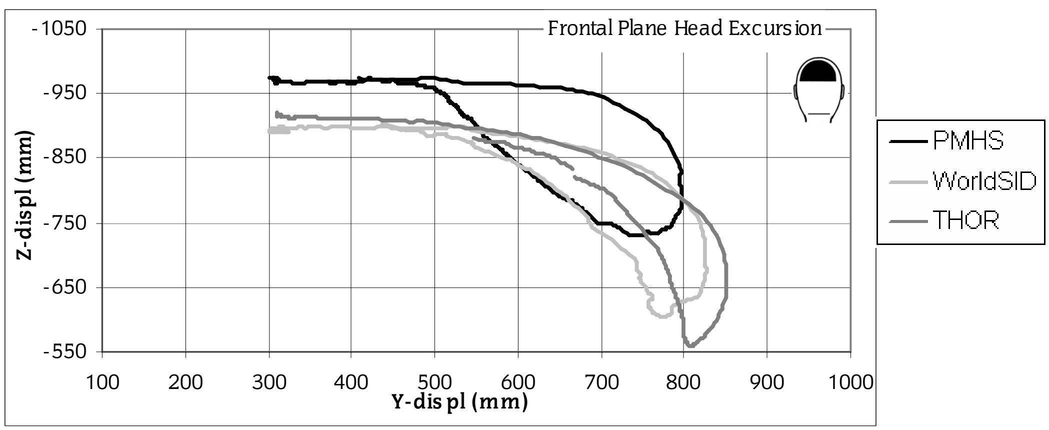

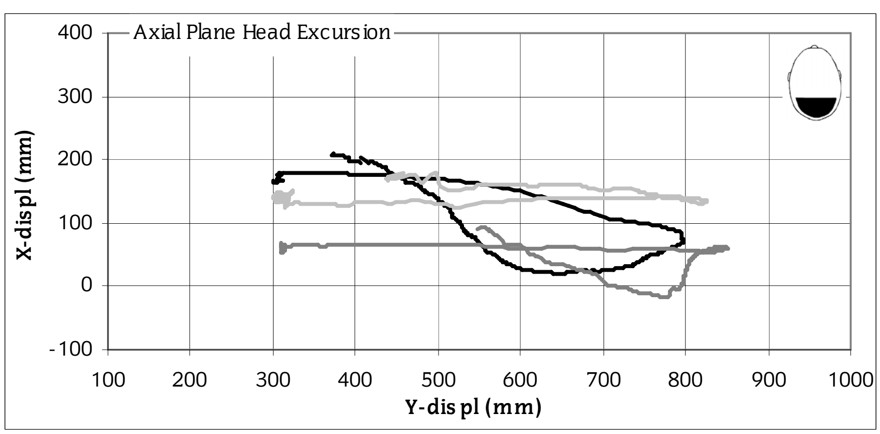

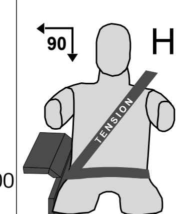

Configuration-1 response curves; high delta-V, 90-degree, outboard shoulder belt-Pretension. Time axis is in milliseconds. Head excursion measures are relative to seat reference frame.

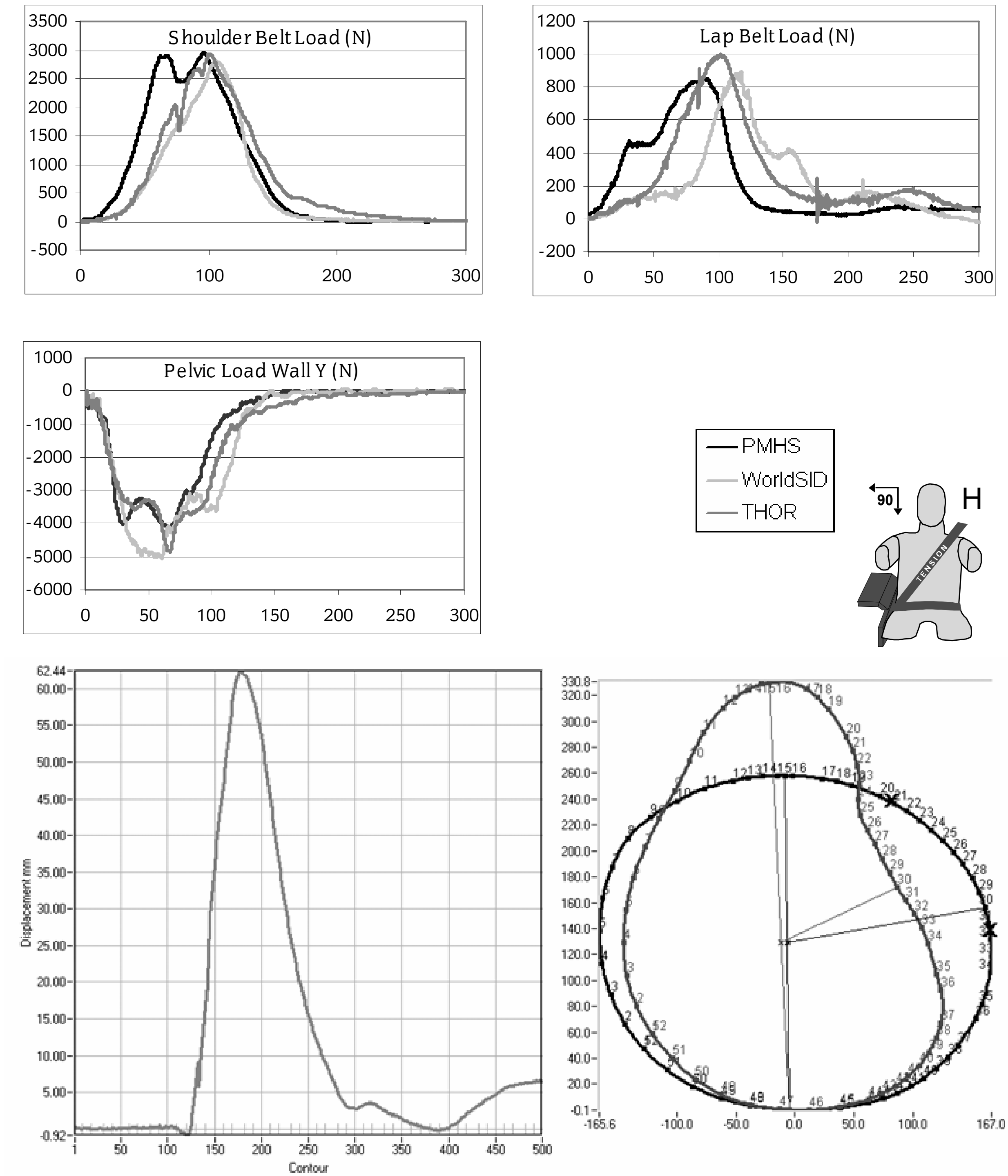

Configuration-1 response curves; high delta-V, 90-degree, outboard shoulder belt-Pretension. Time axis is in milliseconds. Chestband contours are from the PMHS test with "X" marks where equivalent dummy recordings would be.

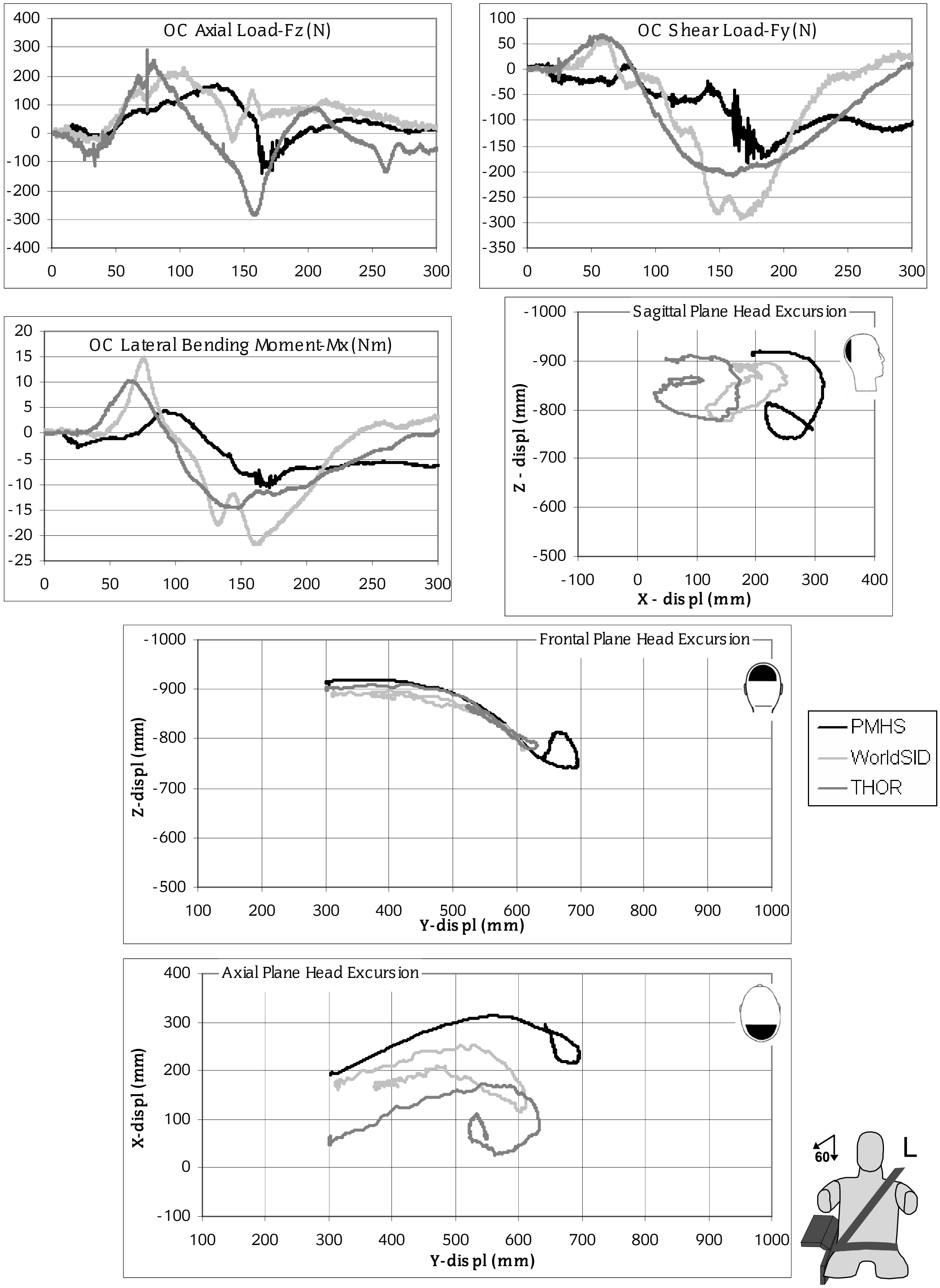

Configuration-2 response curves; low delta-V, 60-degree, outboard shoulder belt. Time axis is in milliseconds. Head excursion measures are relative to seat reference frame.

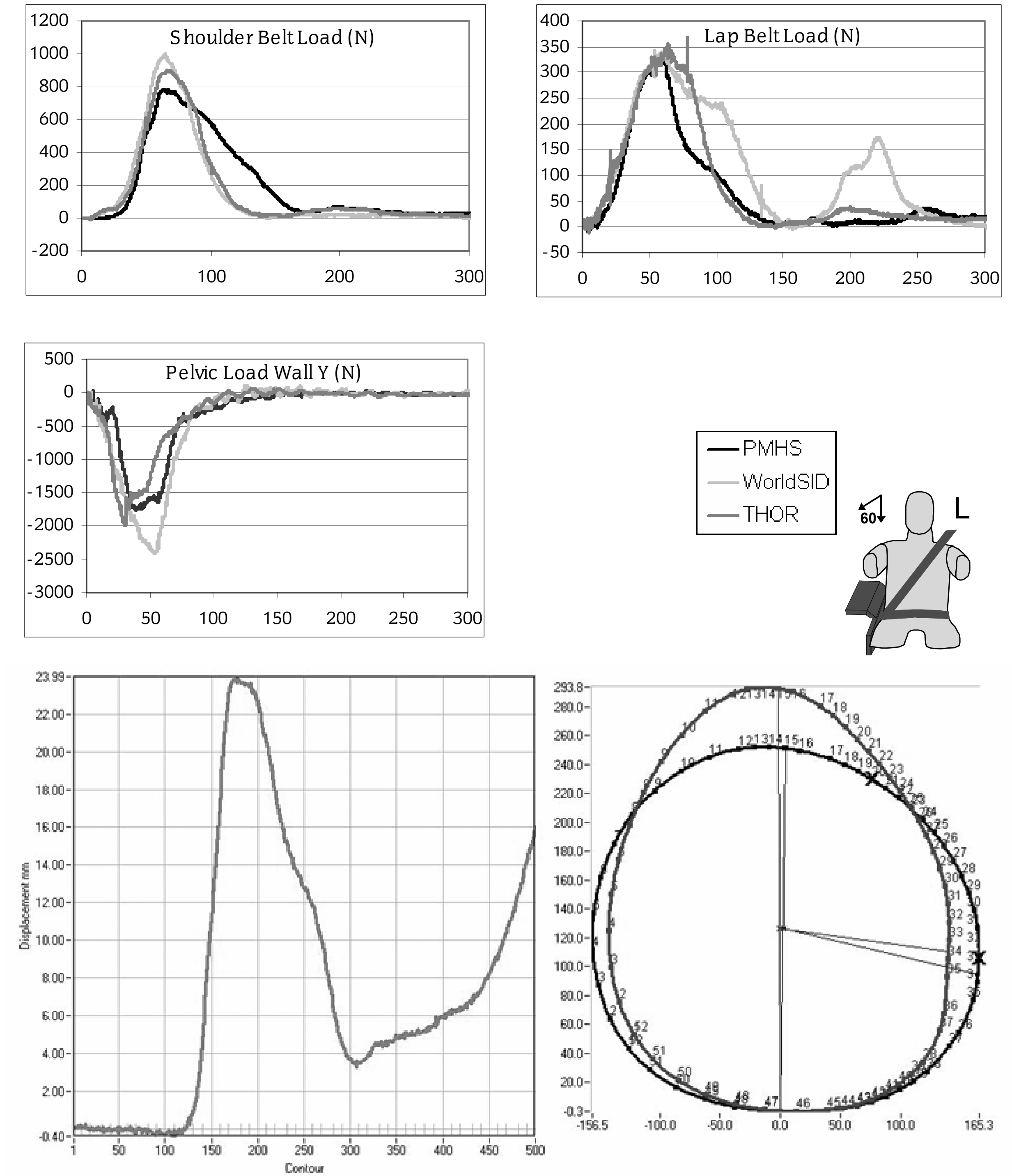

Configuration-2 response curves; low delta-V, 60-degree, outboard shoulder belt. Time axis is in milliseconds. Chestband contours are from the PMHS test with "X" marks where equivalent dummy recordings would be.

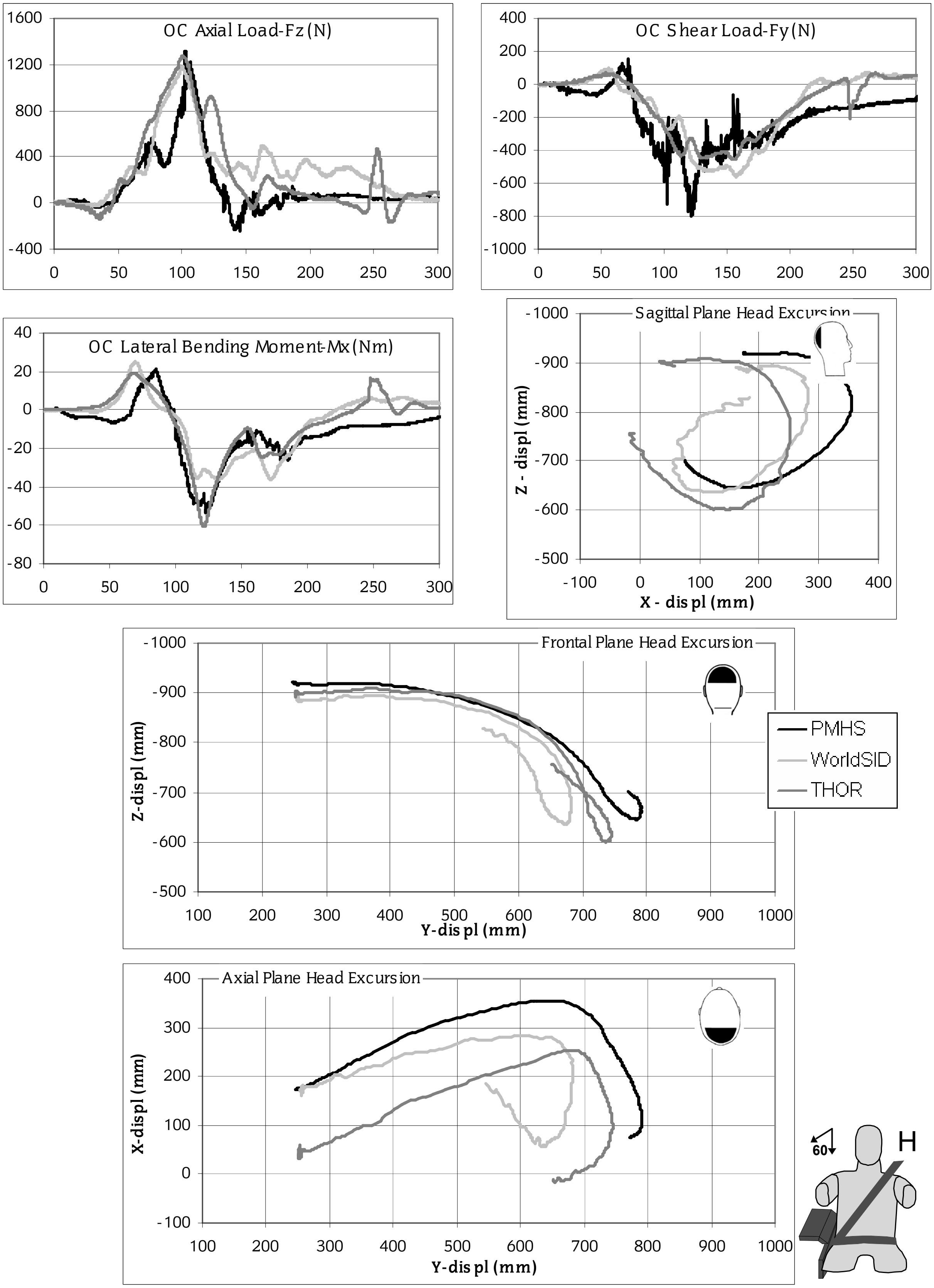

Configuration-3 response curves; high delta-V, 60-degree, outboard shoulder belt. Time axis is in milliseconds. Head excursion measures are relative to seat reference frame.

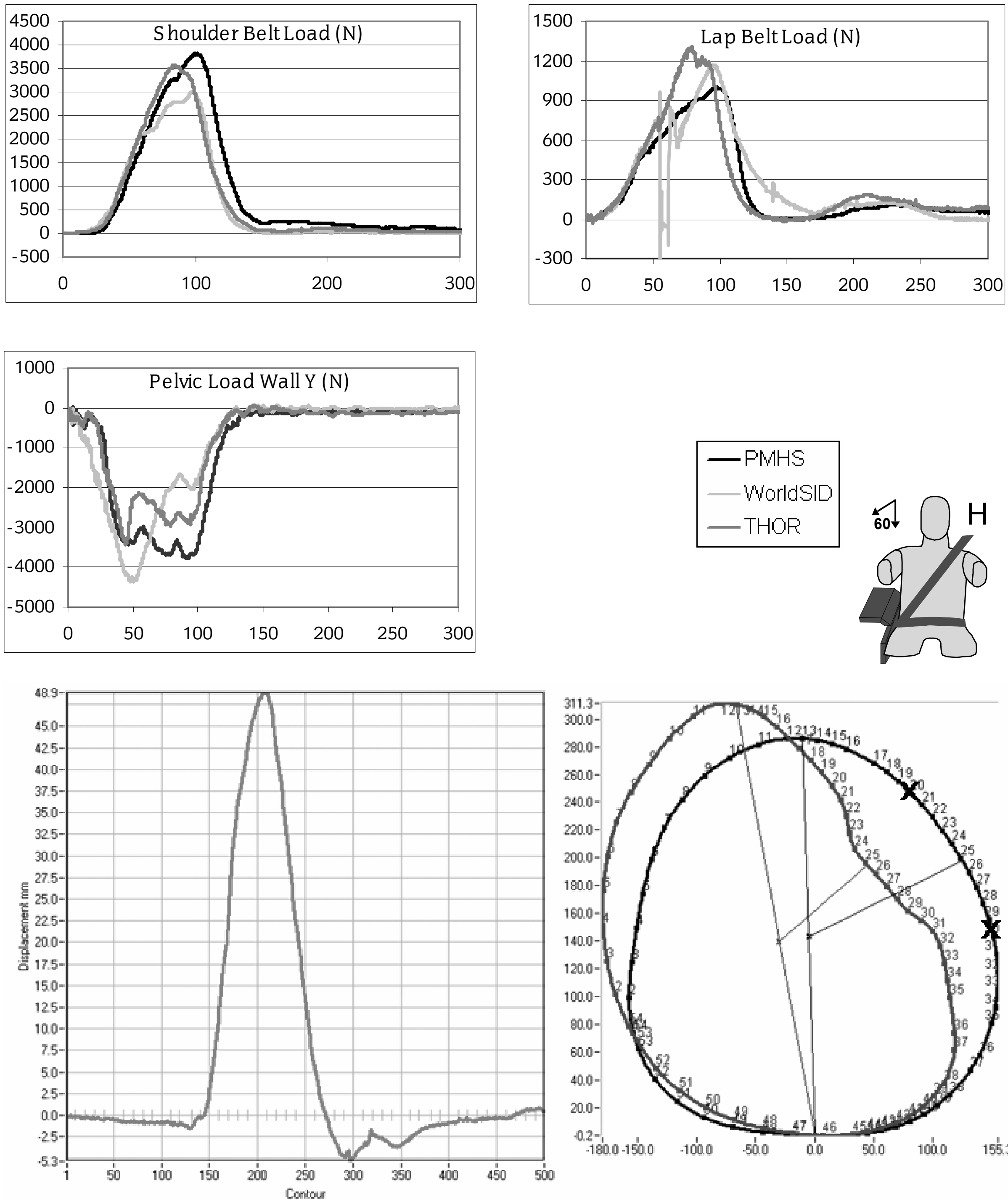

Configuration-3 response curves; high delta-V, 60-degree, outboard shoulder belt. Time axis is in milliseconds. Chestband contours are from the PMHS test with “X” marks where equivalent dummy recordings would be.

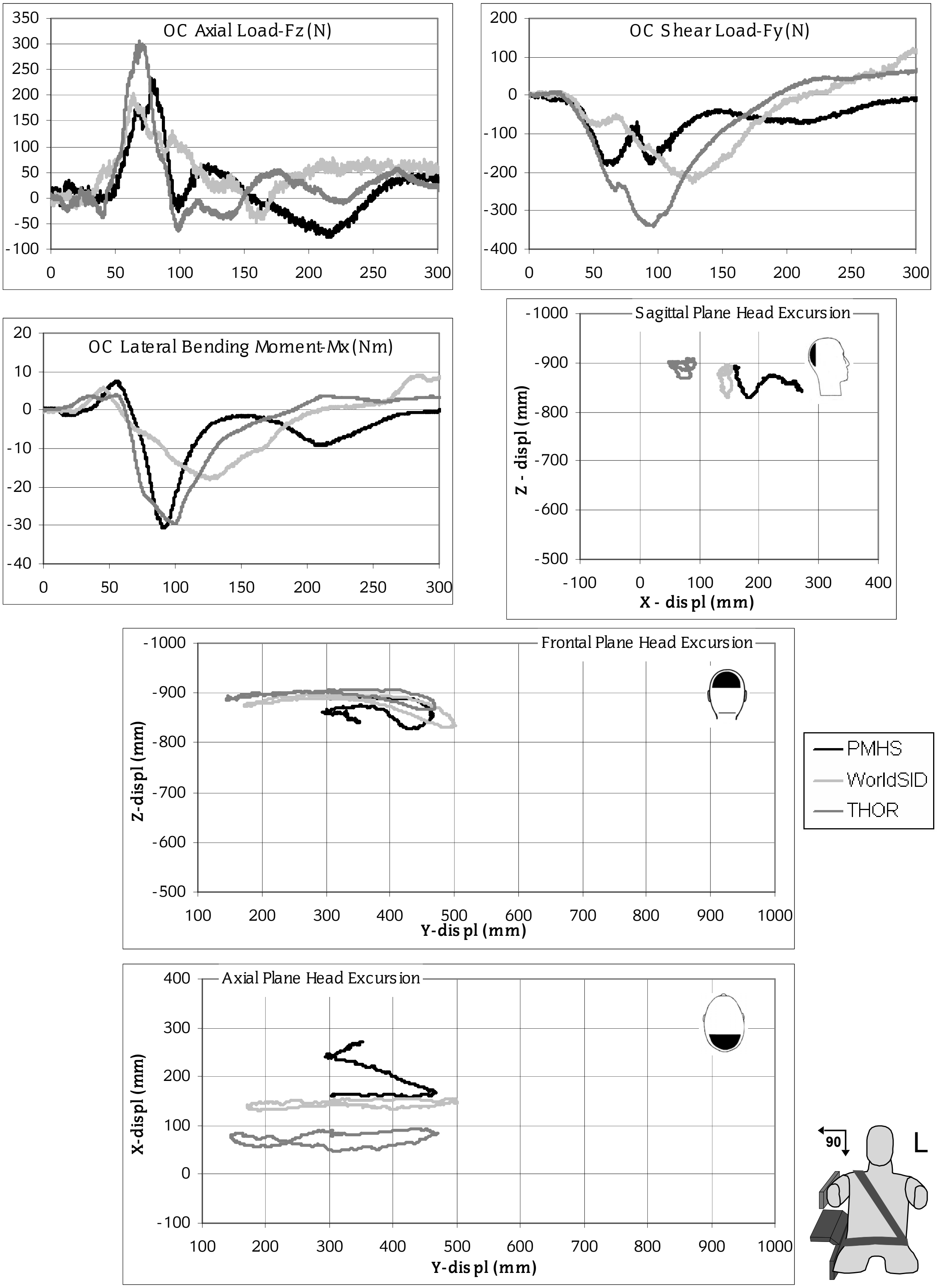

Configuration-4 response curves; low delta-V, 90-degree, shoulder plate, inboard shoulder belt, low belt position. Time axis is in milliseconds. Head excursion measures are relative to seat reference frame.

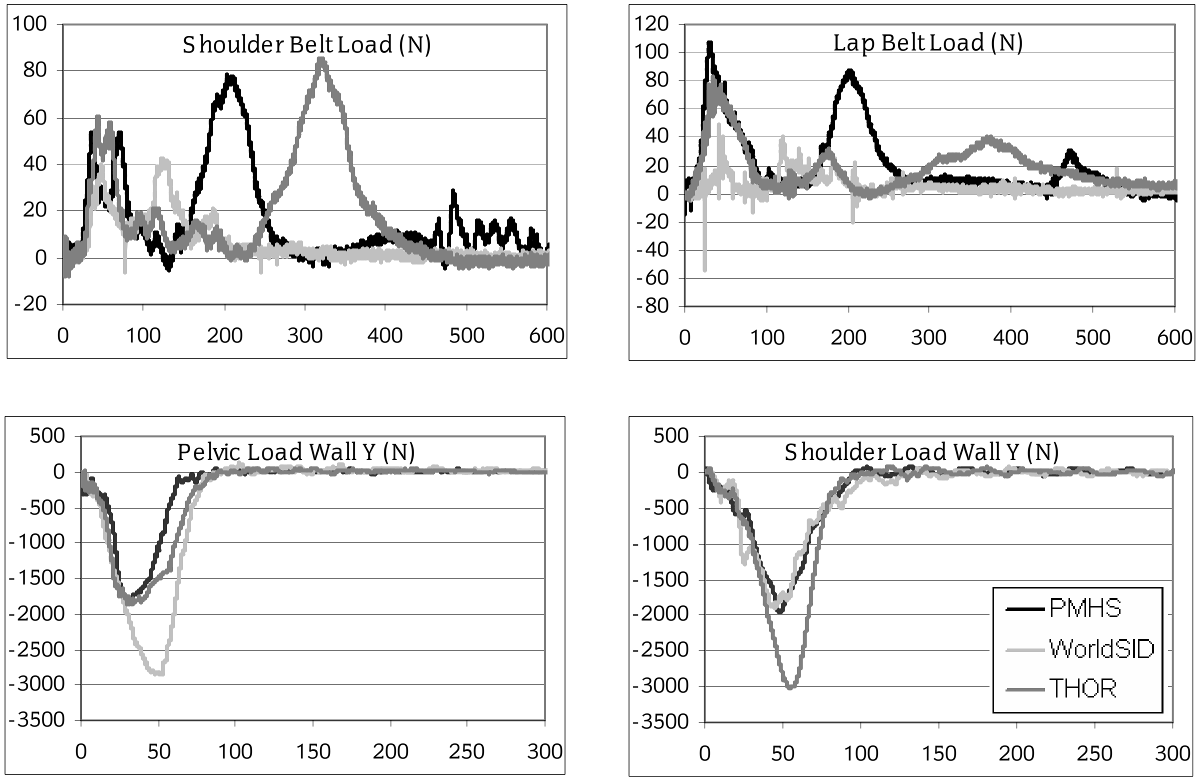

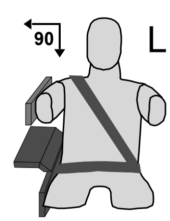

Configuration-4 response curves; low delta-V, 90-degree, shoulder plate, inboard shoulder belt, low belt position. Time axis is in milliseconds.

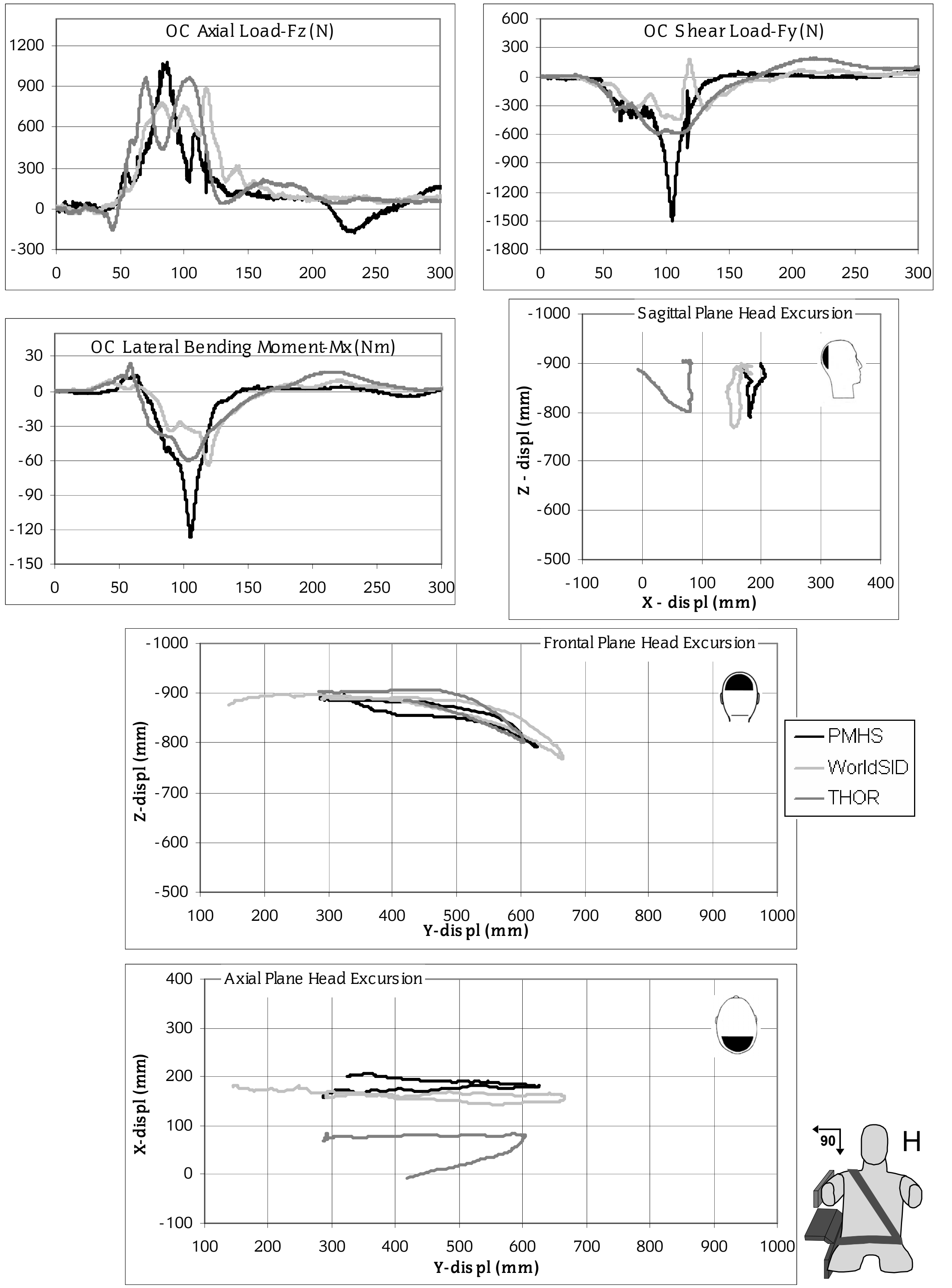

Configuration-5 response curves; high delta-V, 90-degree, shoulder plate, inboard shoulder belt, low belt position. Time axis is in milliseconds. Head excursion measures are relative to seat reference frame.

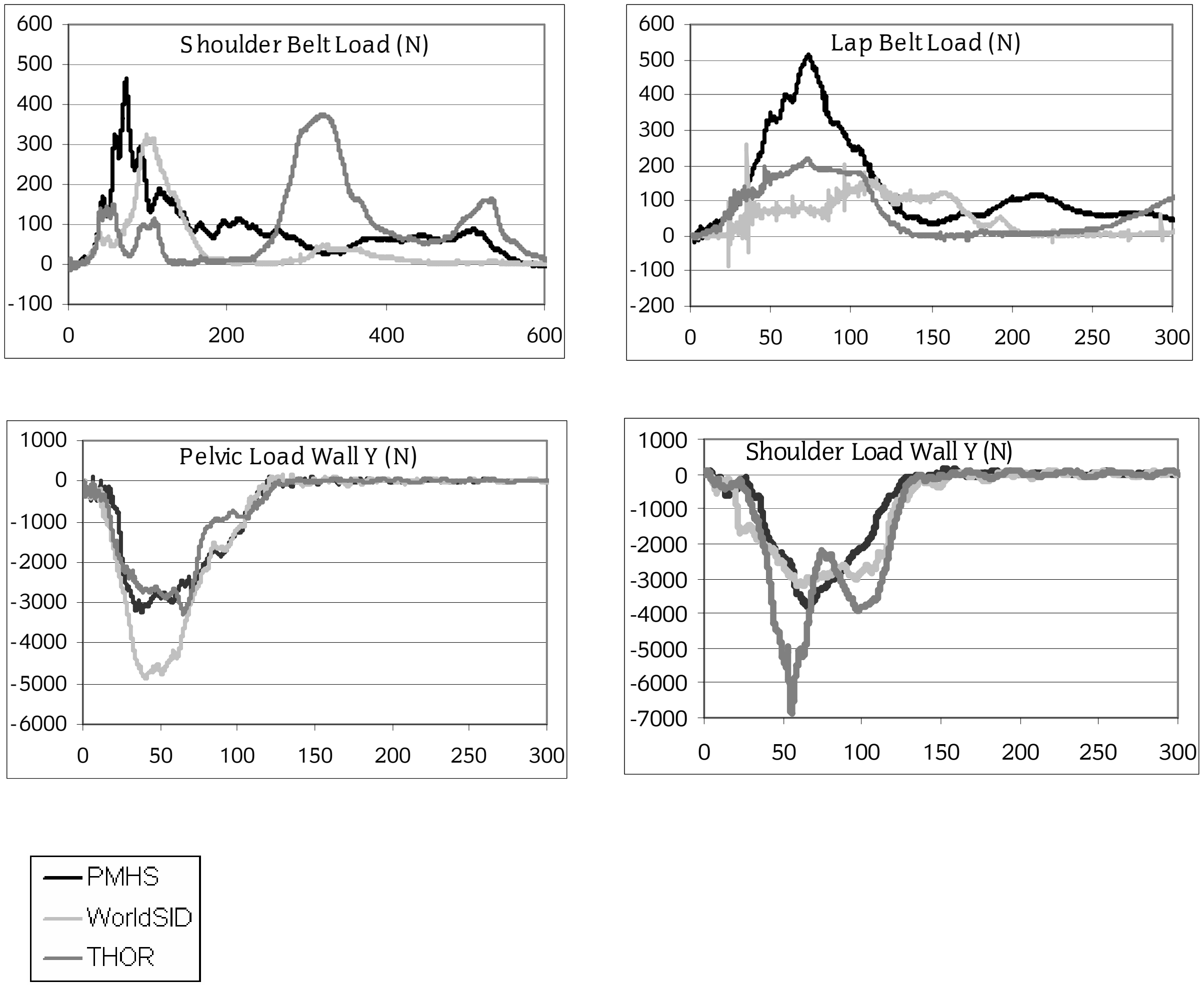

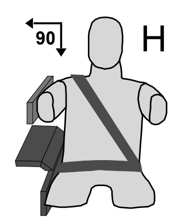

Configuration-5 response curves; high delta-V, 90-degree, shoulder plate, inboard shoulder belt, low belt position. Time axis is in milliseconds.

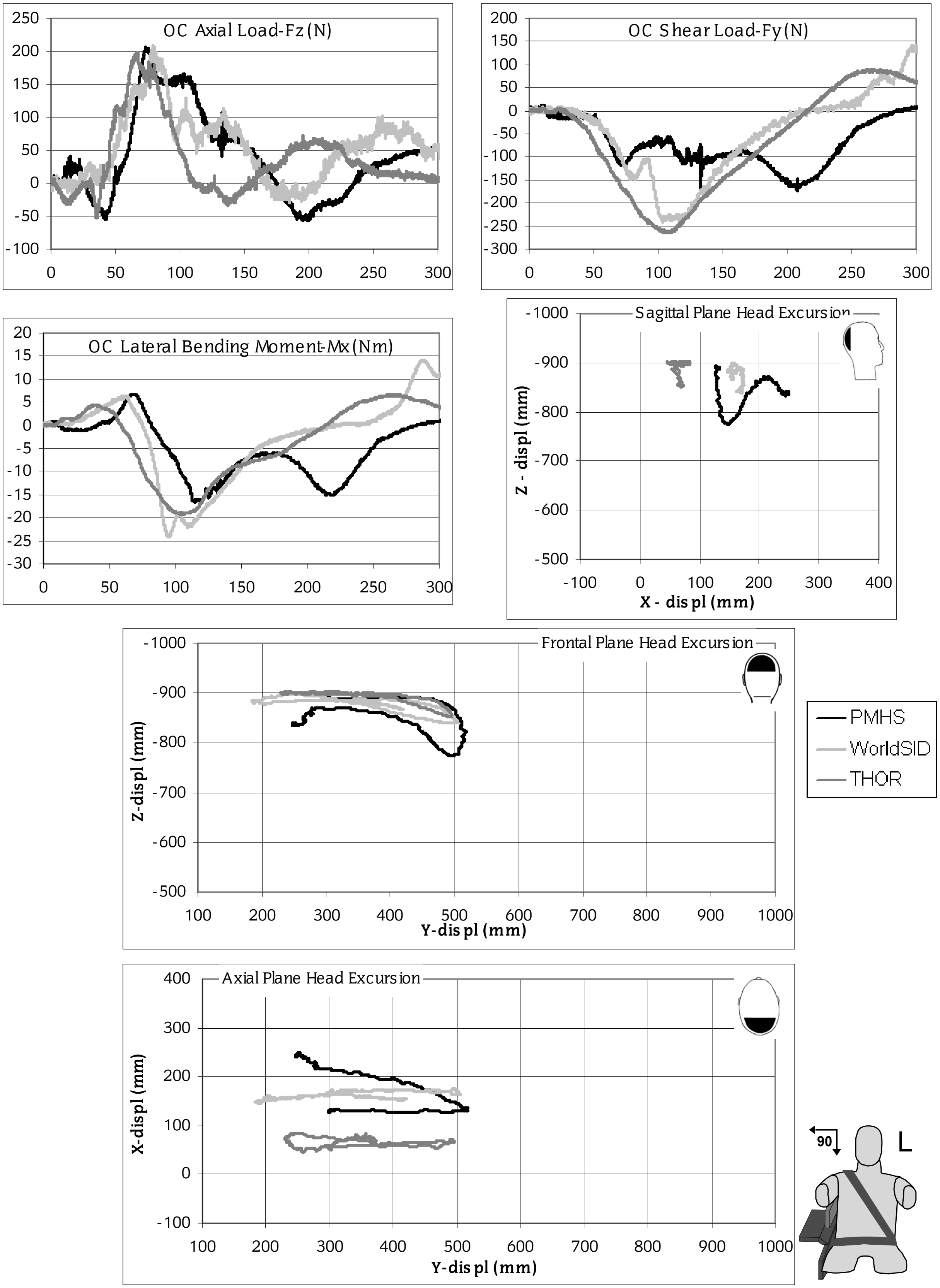

Configuration-6 response curves; low delta-V, 90-degree, thorax plate, inboard shoulder belt, low belt position. Time axis is in milliseconds. Head excursion measures are relative to seat reference frame.

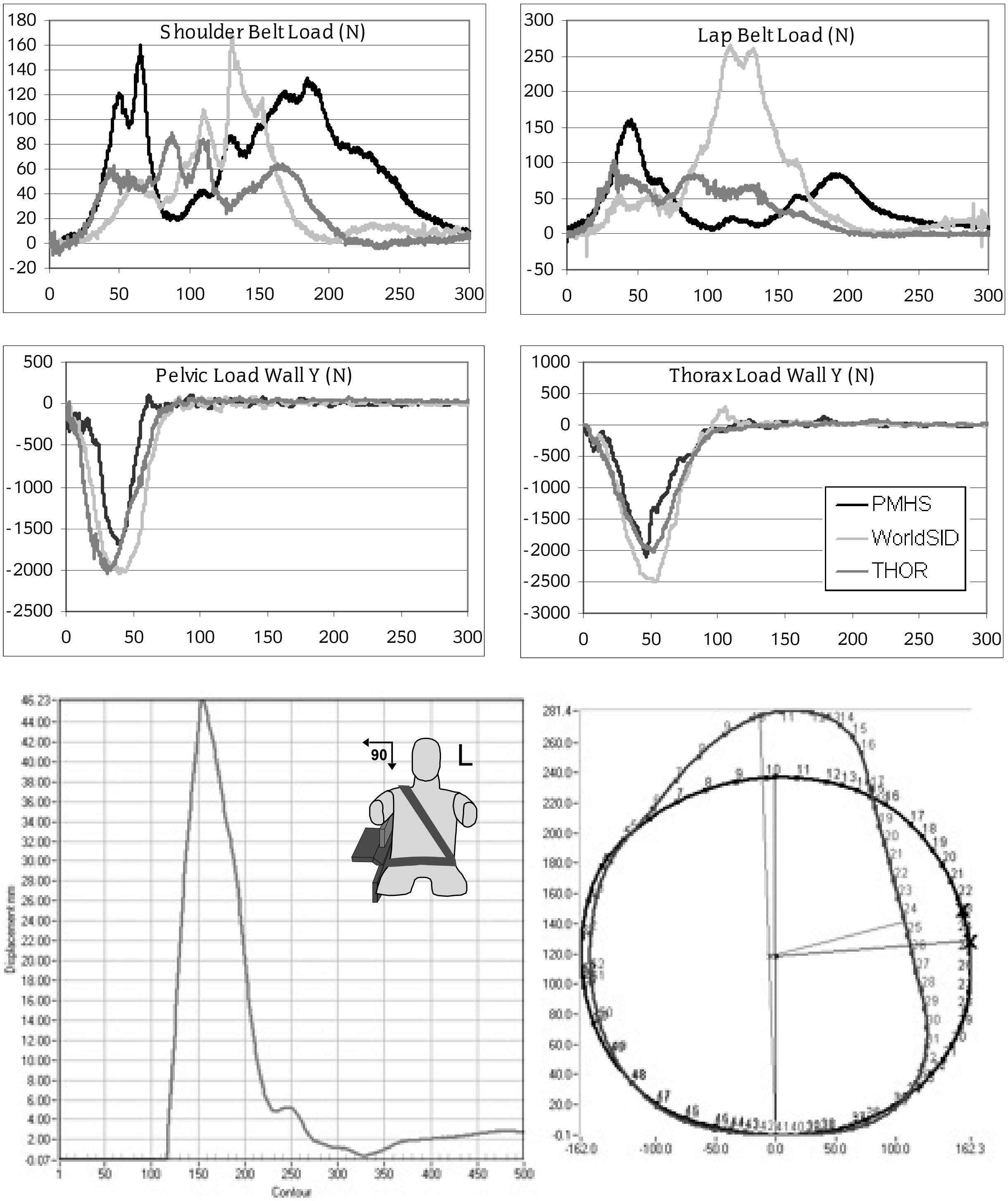

Configuration-6 response curves; low delta-V, 90-degree, thorax plate, inboard shoulder belt, low belt position. Time axis is in milliseconds. Chestband contours are from the PMHS test with "X" marks where equivalent dummy recordings would be.

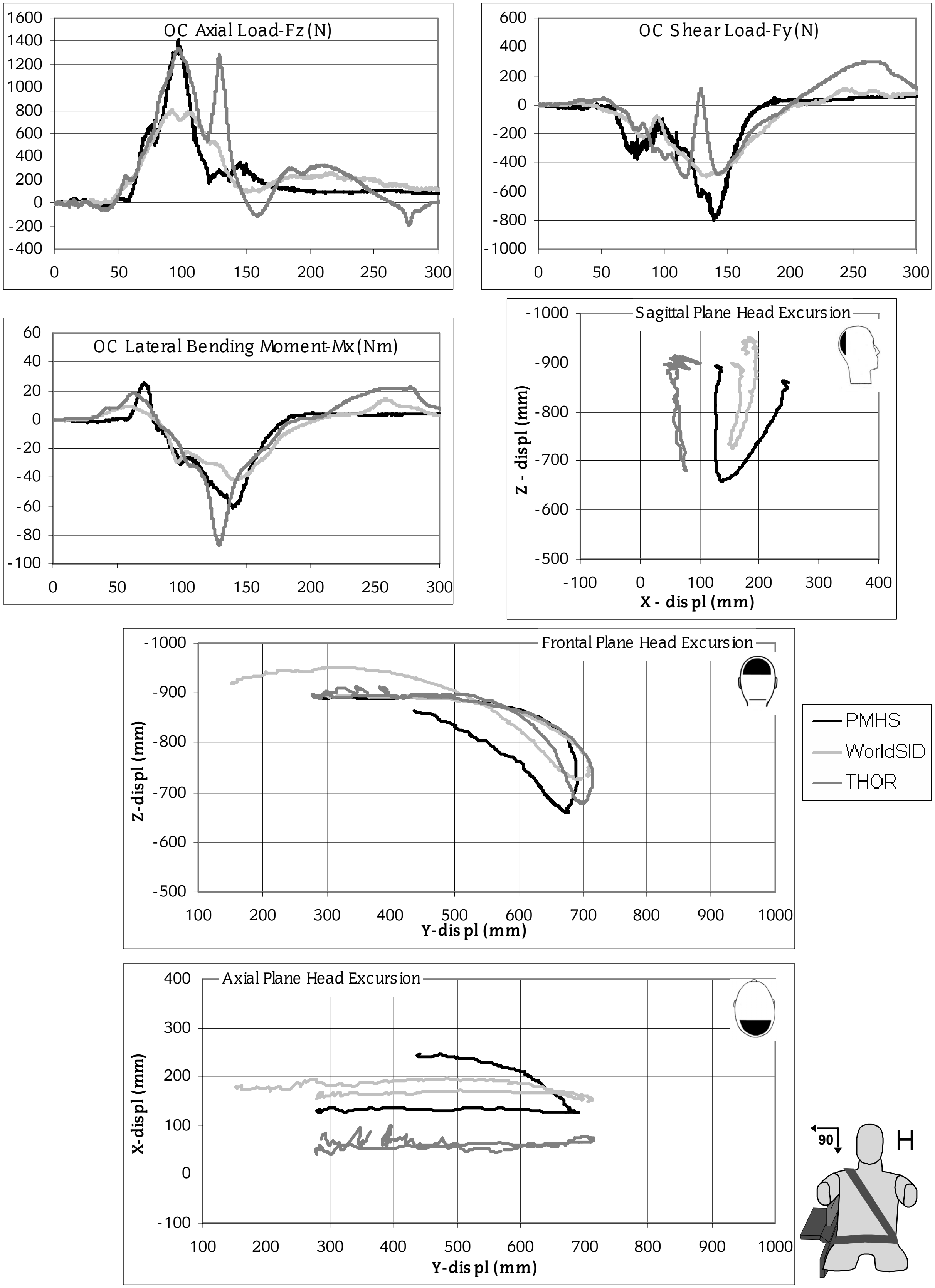

Configuration-7 response curves; high delta-V, 90-degree, thorax plate, inboard shoulder belt, low belt position. Time axis is in milliseconds. Head excursion measures are relative to seat reference frame.

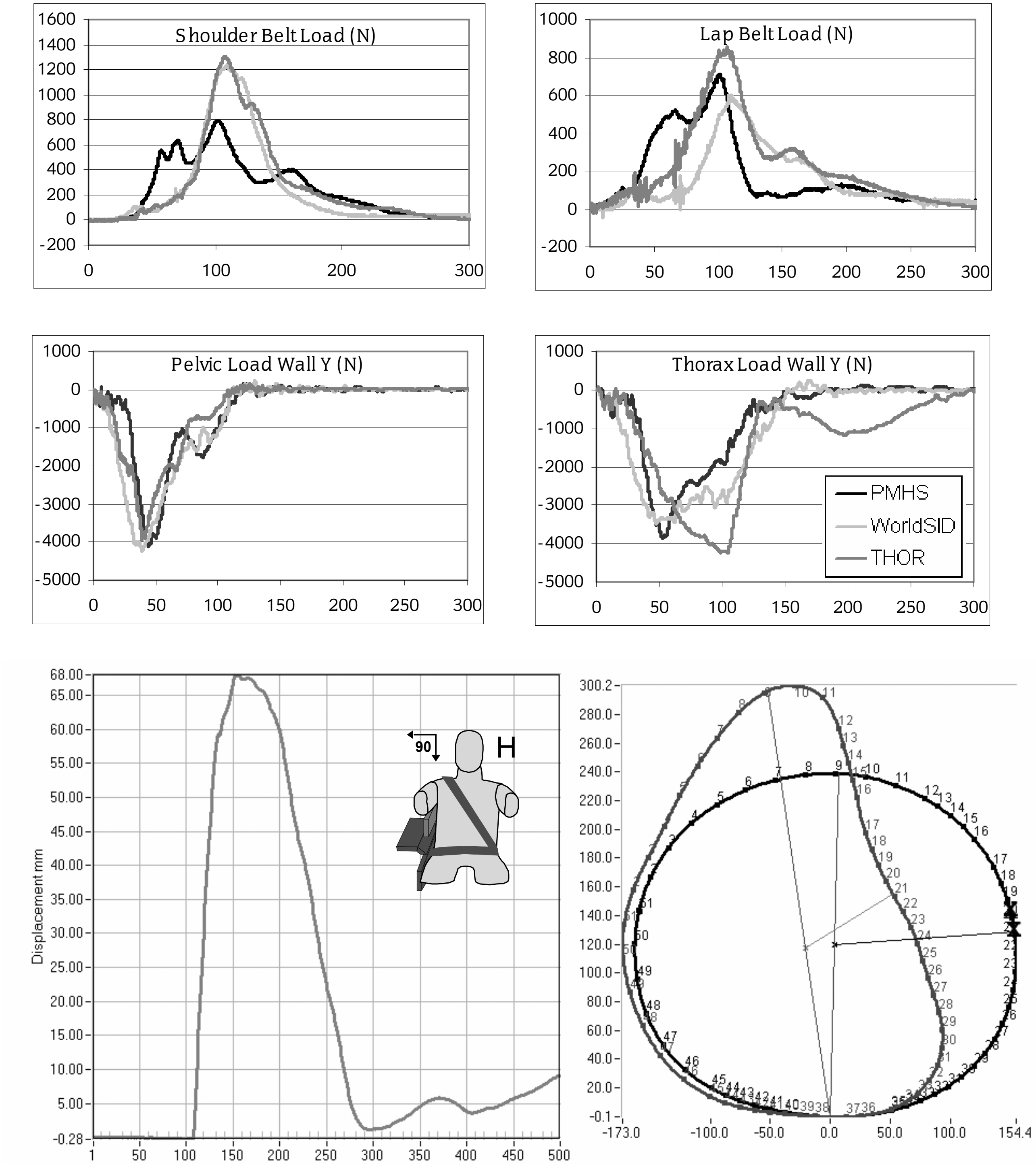

Configuration-7 response curves; high delta-V, 90-degree, thorax plate, inboard shoulder belt, low belt position. Time axis is in milliseconds. Chestband contours are from the PMHS test with "X" marks where equivalent dummy recordings would be.

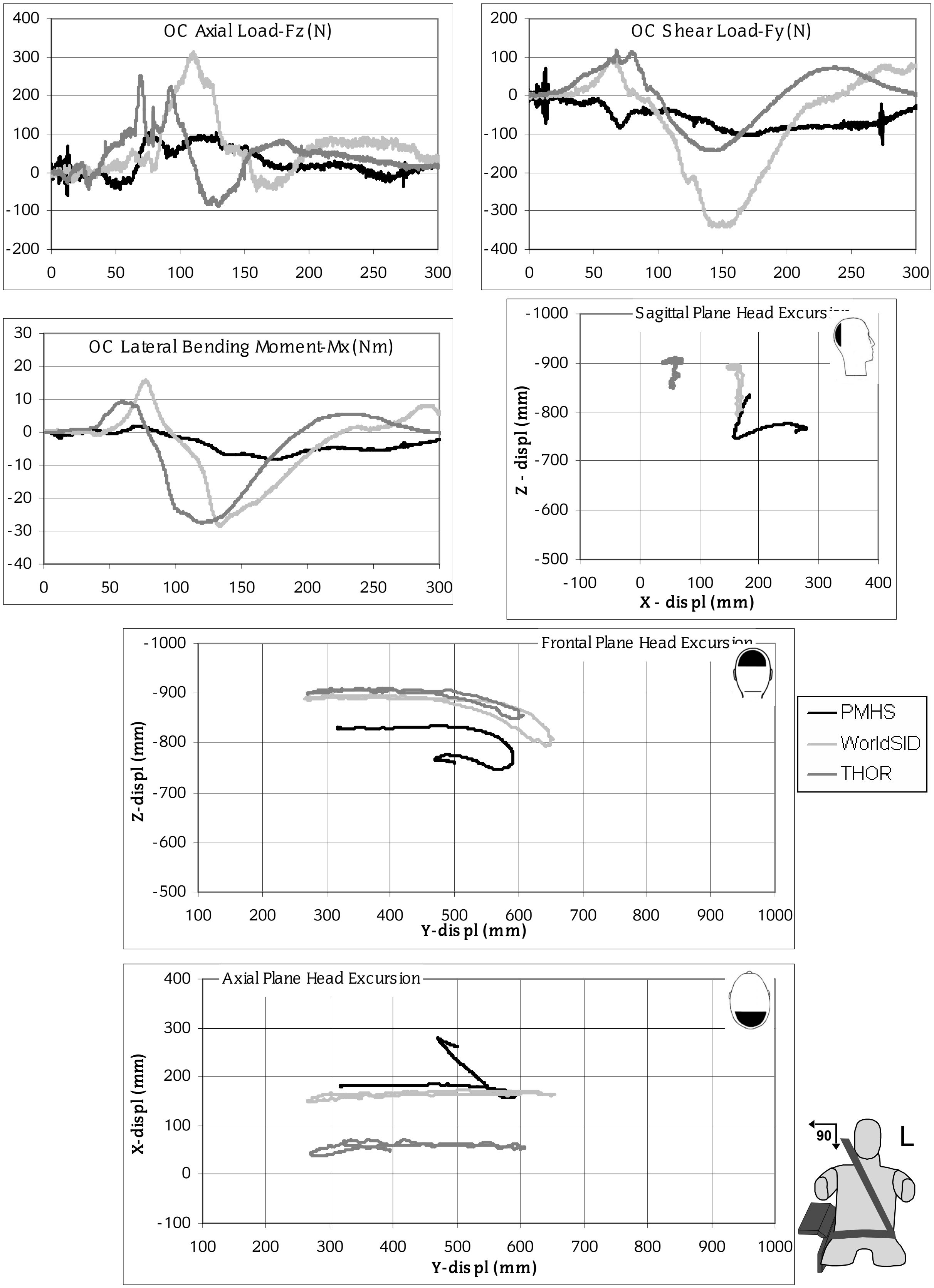

Configuration-8 response curves; low delta-V, 90-degree, inboard shoulder belt, high belt position. Time axis is in milliseconds. Head excursion measures are relative to seat reference frame.

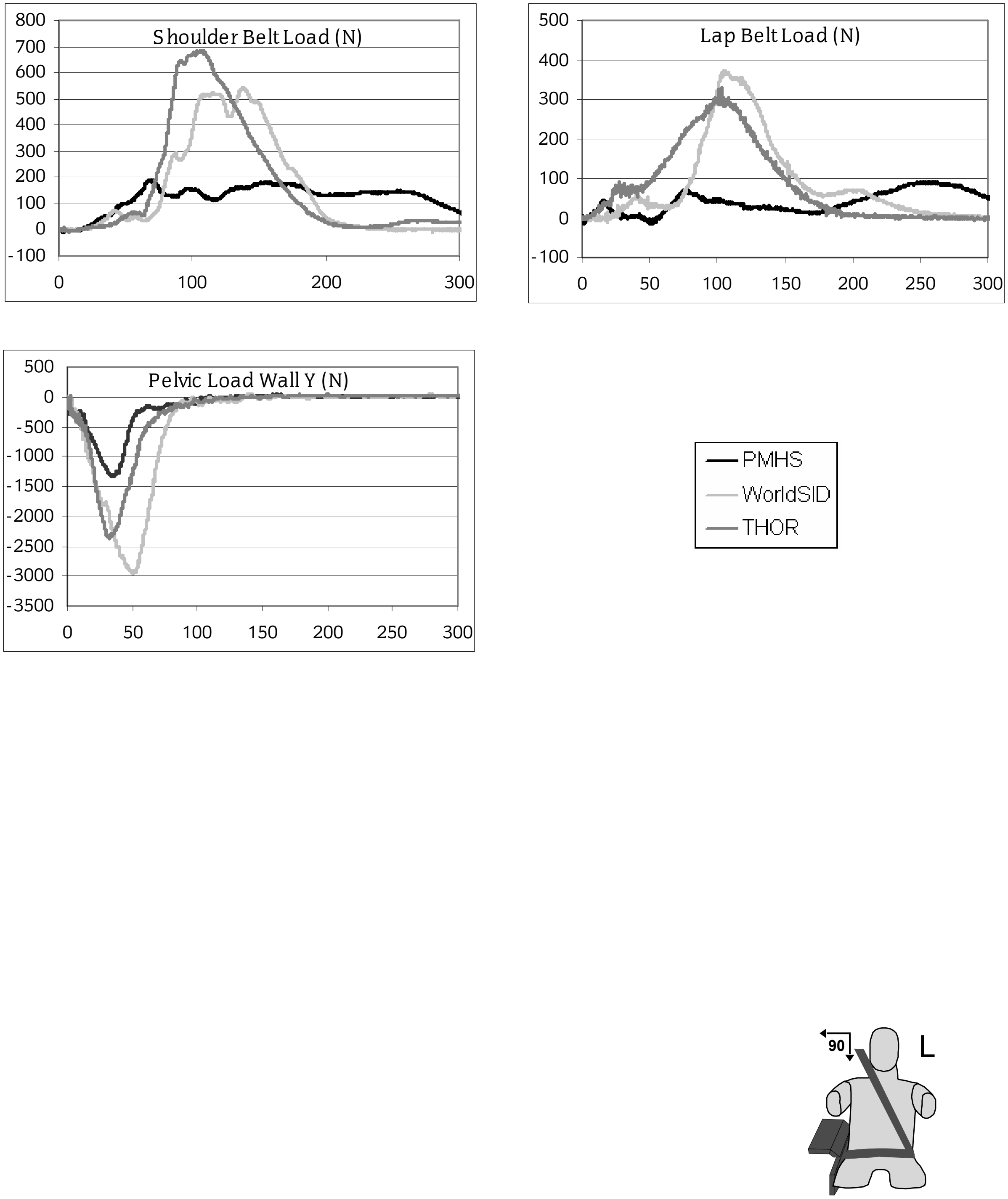

Configuration-8 response curves; low delta-V, 90-degree, inboard shoulder belt, high belt position. Time axis is in milliseconds.

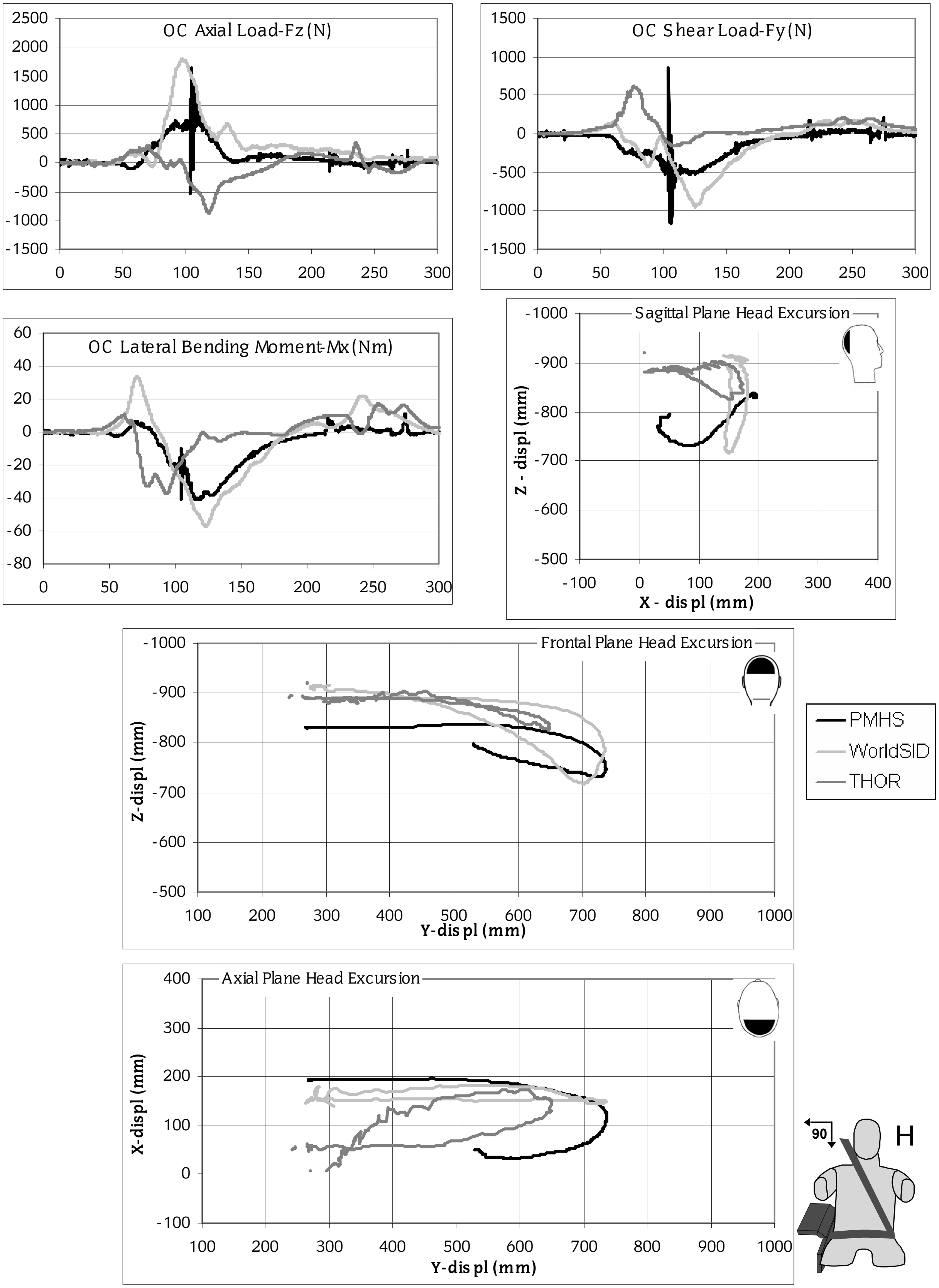

Configuration-9 response curves; high delta-V, 90-degree, inboard shoulder belt, high belt position. Time axis is in milliseconds. Head excursion measures are relative to seat reference frame.

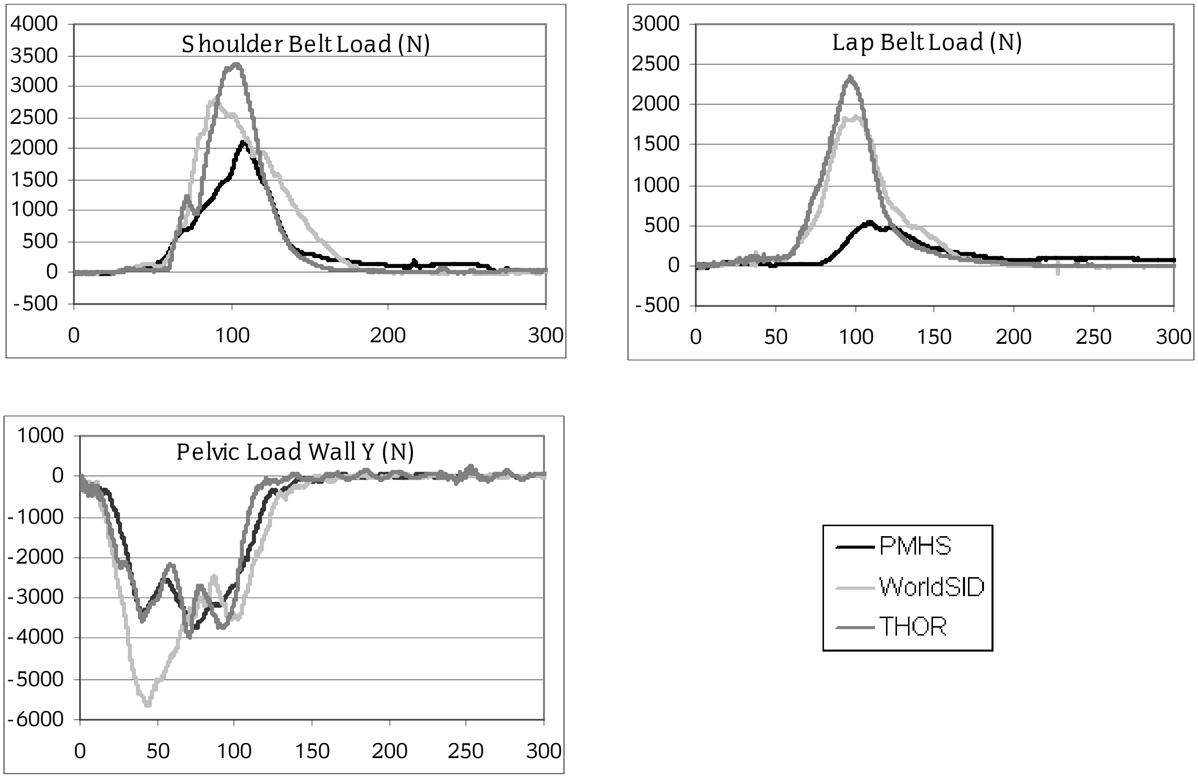

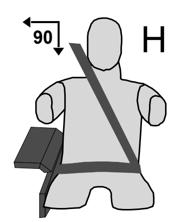

Configuration-9 response curves; high delta-V, 90-degree, inboard shoulder belt, high belt position. Time axis is in milliseconds.

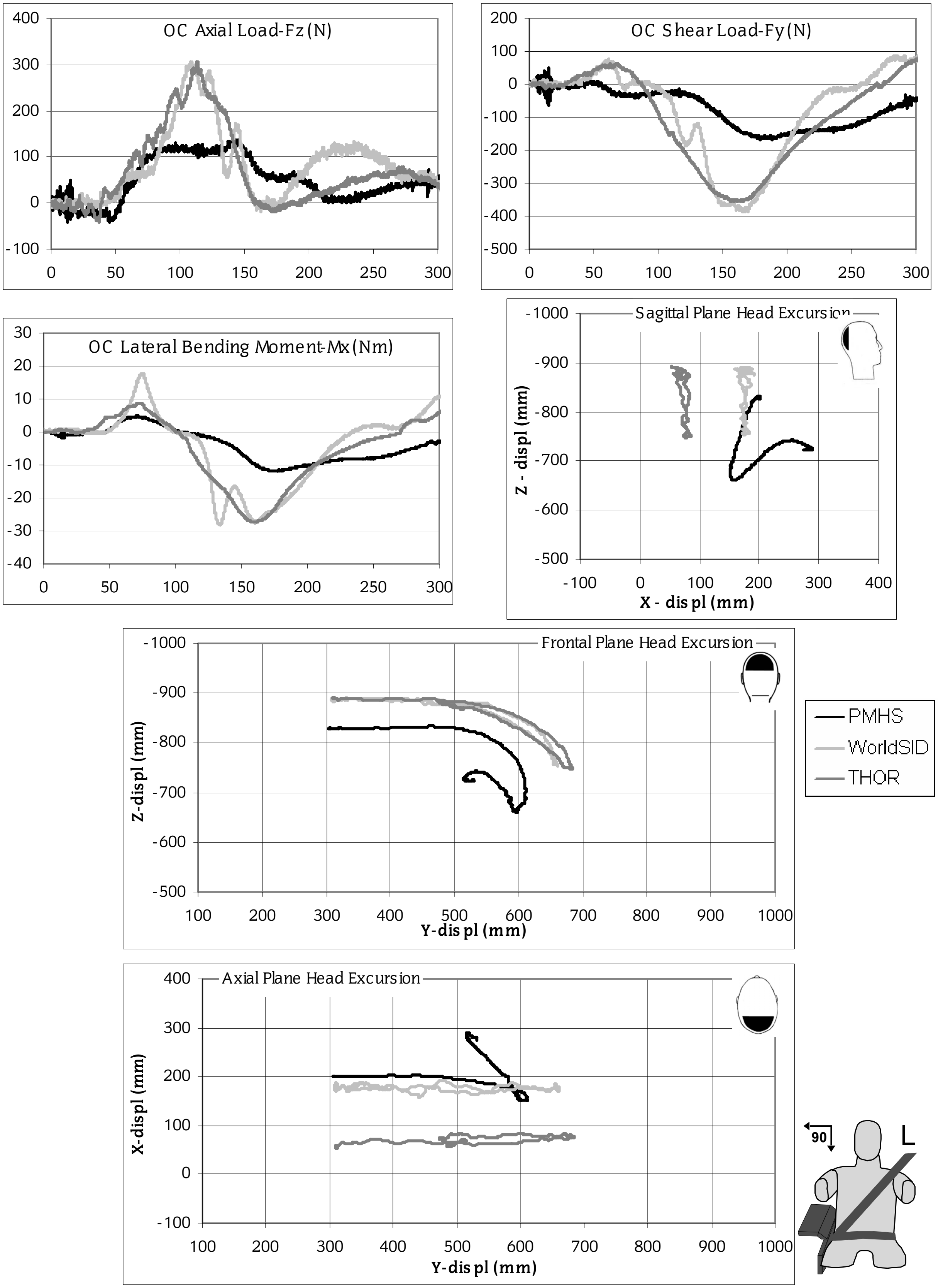

Configuration-10 response curves; low delta-V, 90-degree, outboard shoulder belt, forward D-ring position. Time axis is in milliseconds. Head excursion measures are relative to seat reference frame.

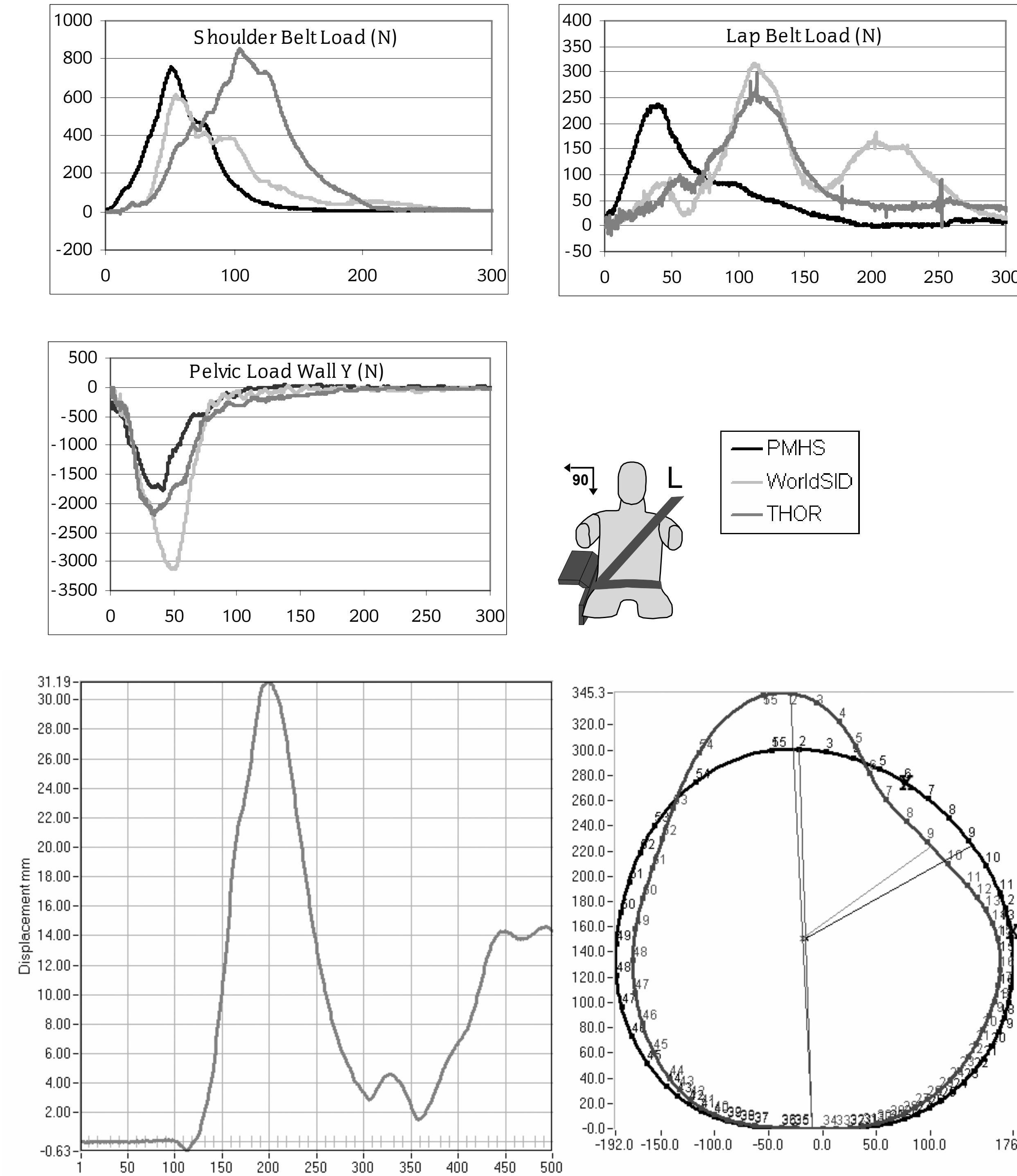

Configuration-10 response curves; low delta-V, 90-degree, outboard shoulder belt, forward D-ring position. Time axis is in milliseconds. Chestband contours are from the PMHS test with “X” marks where equivalent dummy recordings would be.

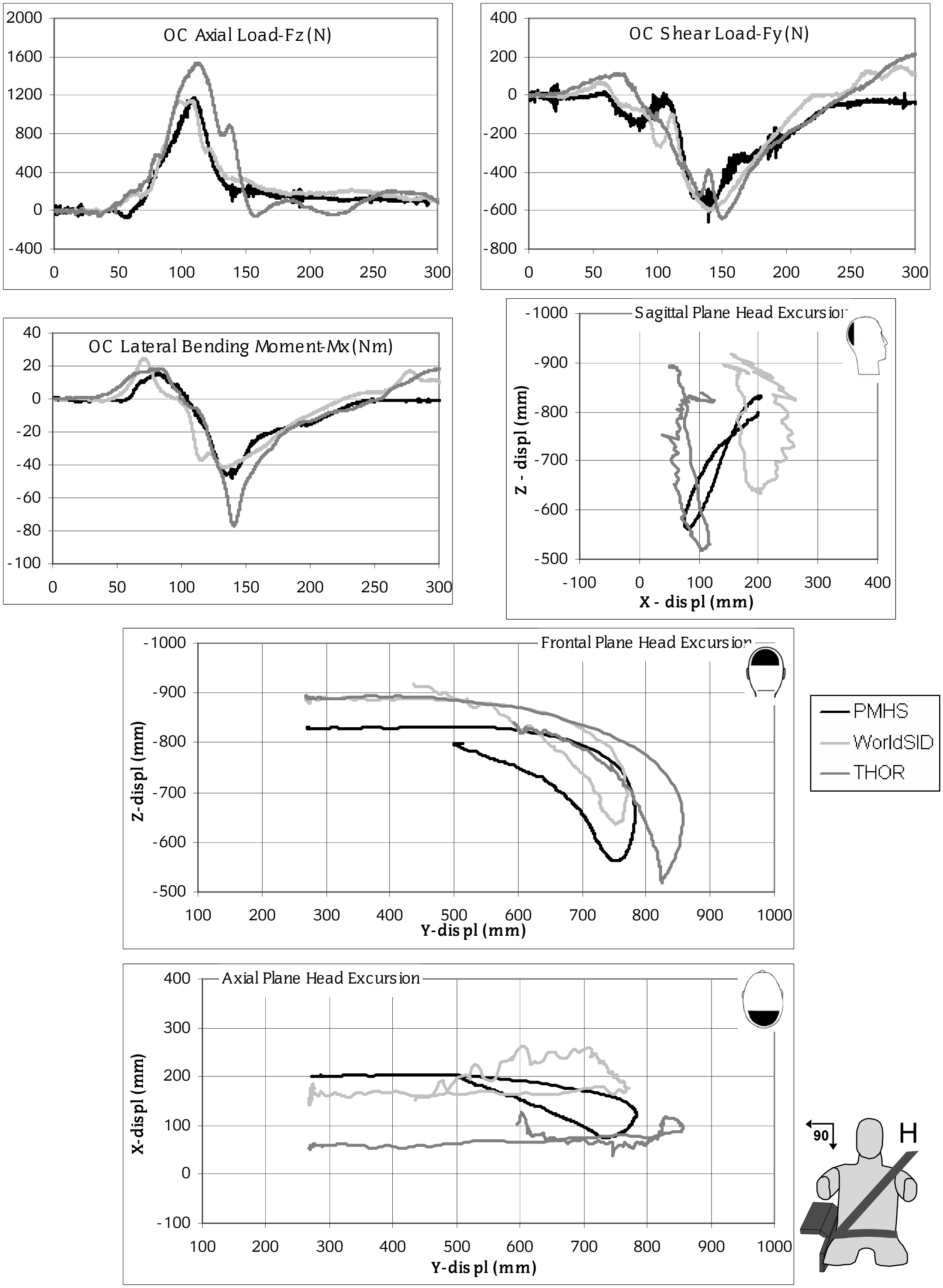

Configuration-11 response curves; high delta-V, 90-degree, outboard shoulder belt, forward D-ring position. Time axis is in milliseconds. Head excursion measures are relative to seat reference frame.

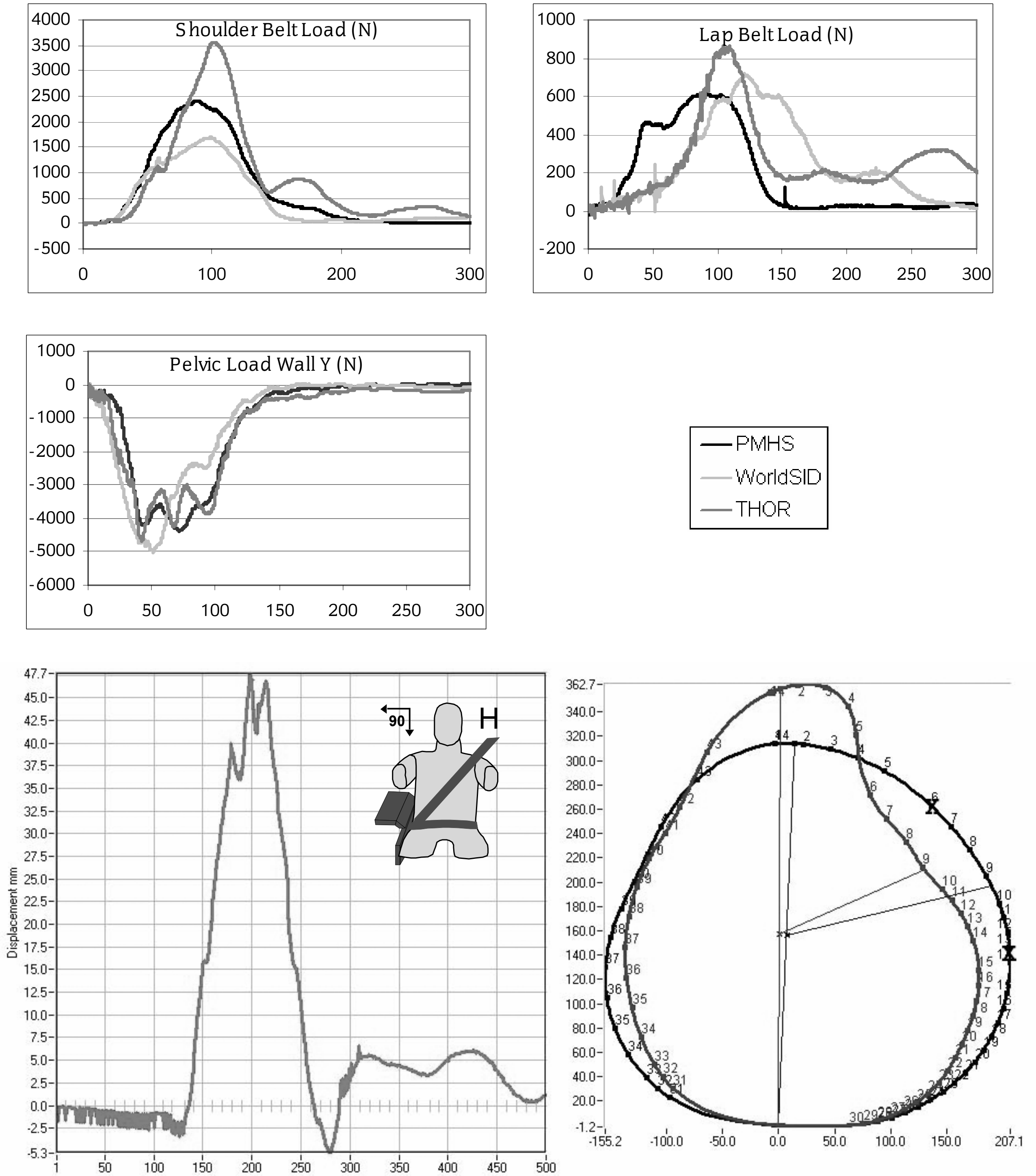

Configuration-11 response curves; high delta-V, 90-degree, outboard shoulder belt, forward D-ring position. Time axis is in milliseconds. Chestband contours are from the PMHS test with “X” marks where equivalent dummy recordings would be.

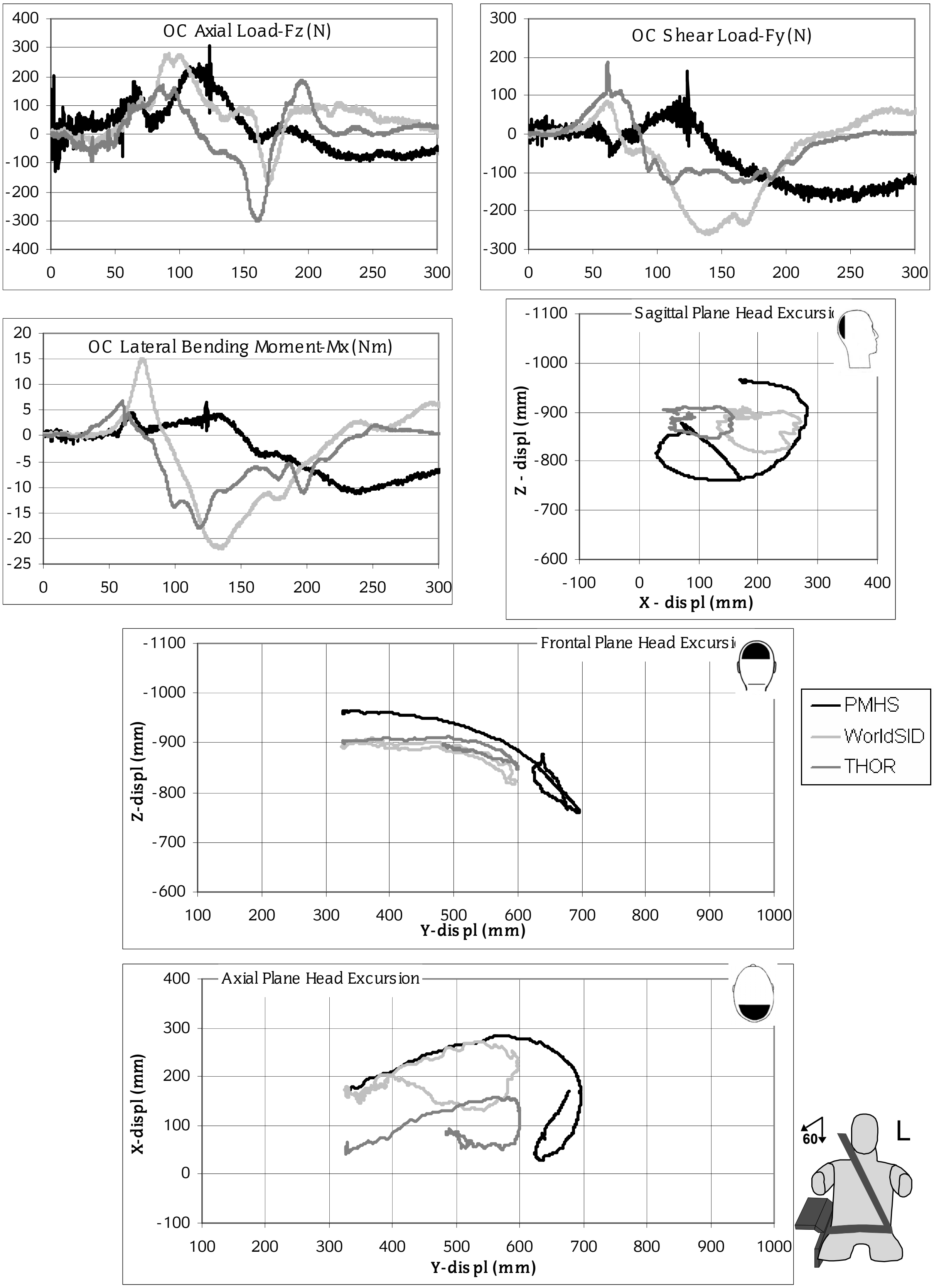

Configuration-14 response curves; low delta-V, 60-degree, inboard shoulder belt, high belt position. Time axis is in milliseconds. Head excursion measures are relative to seat reference frame.

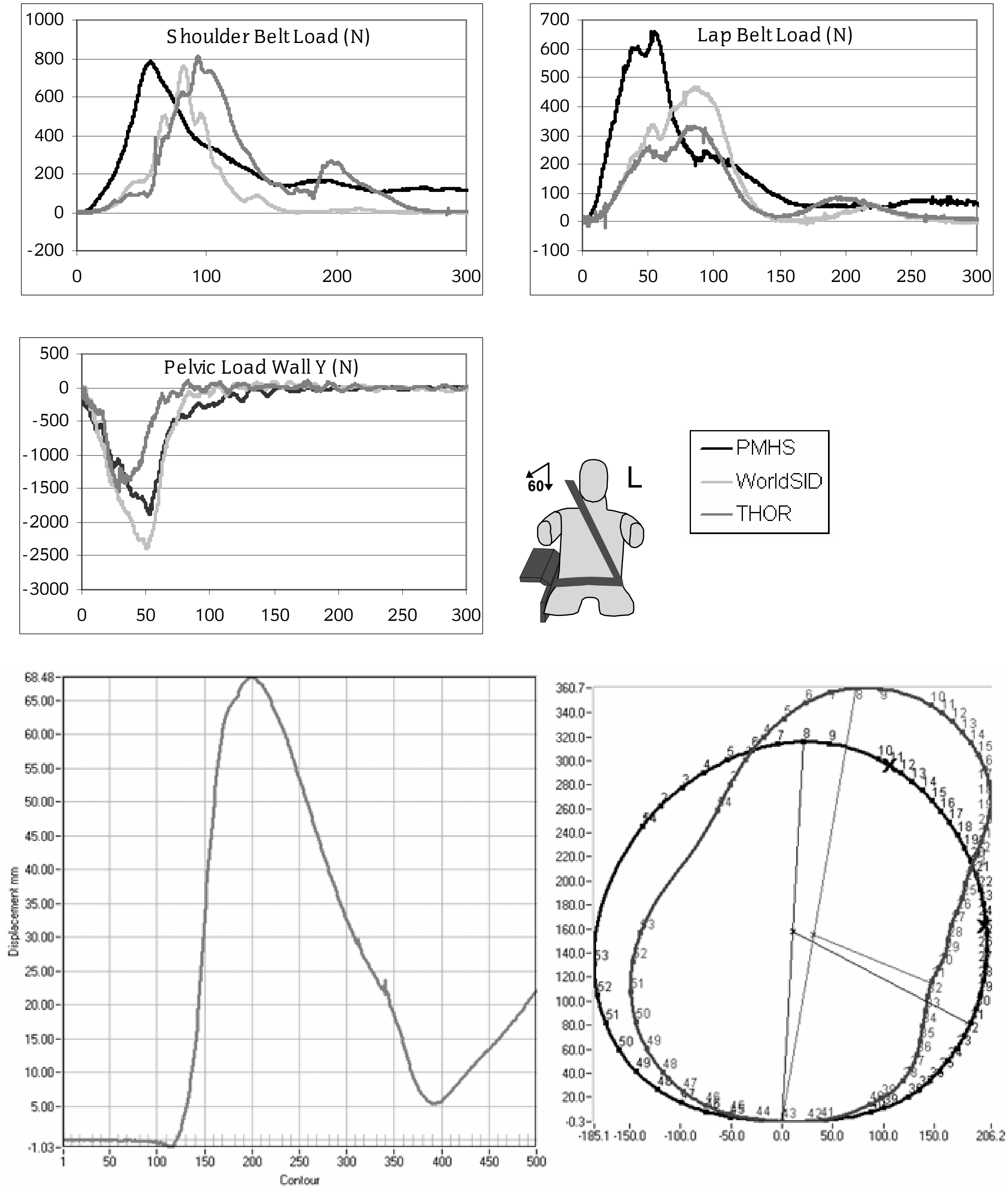

Configuration-14 response curves; low delta-V, 60-degree, inboard shoulder belt, high belt position. Time axis is in milliseconds. Chestband contours are from the PMHS test with "X" marks where equivalent dummy recordings would be.

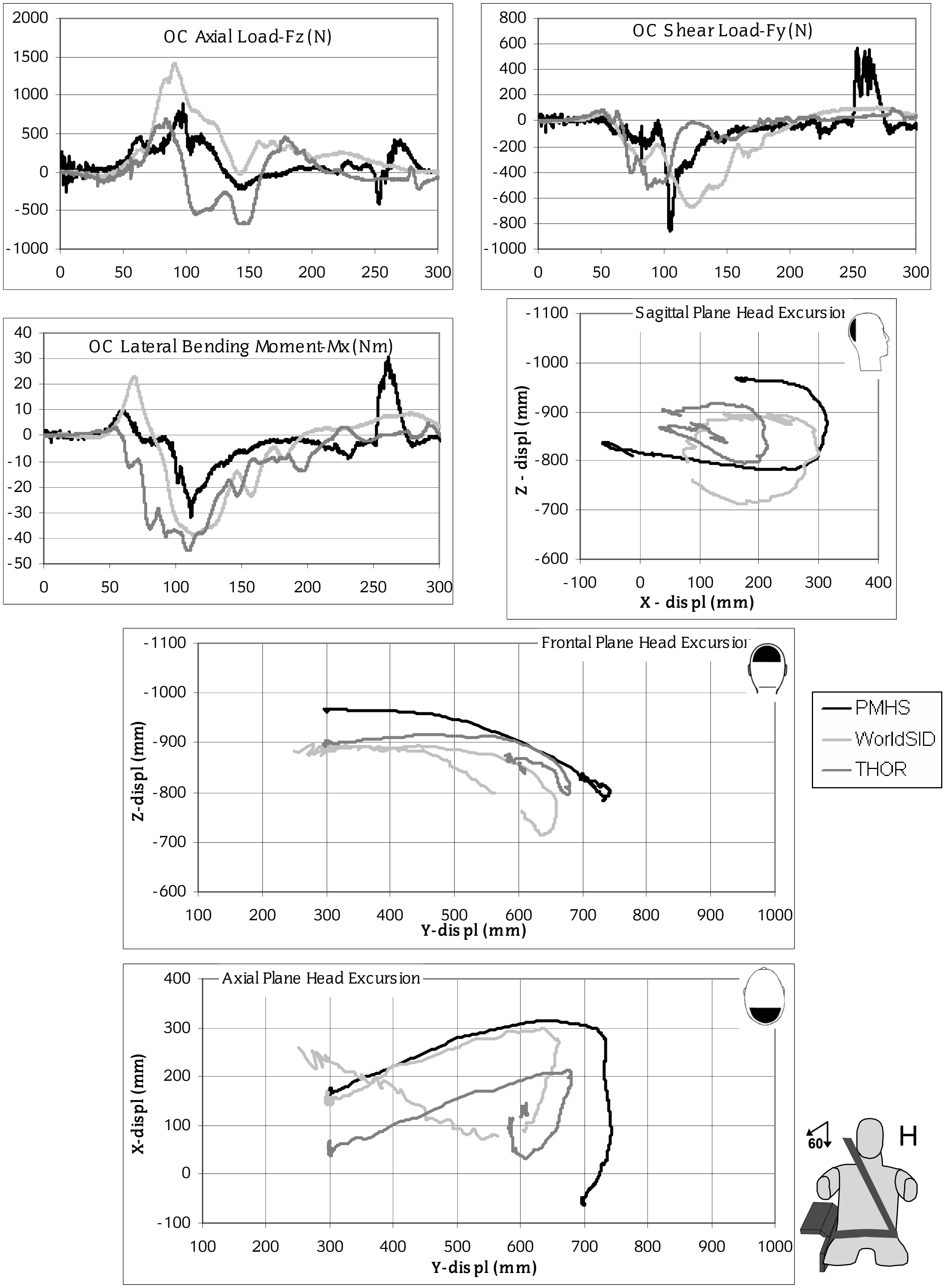

Configuration-15 response curves; high delta-V, 60-degree, inboard shoulder belt, high belt position. Time axis is in milliseconds. Head excursion measures are relative to seat reference frame.

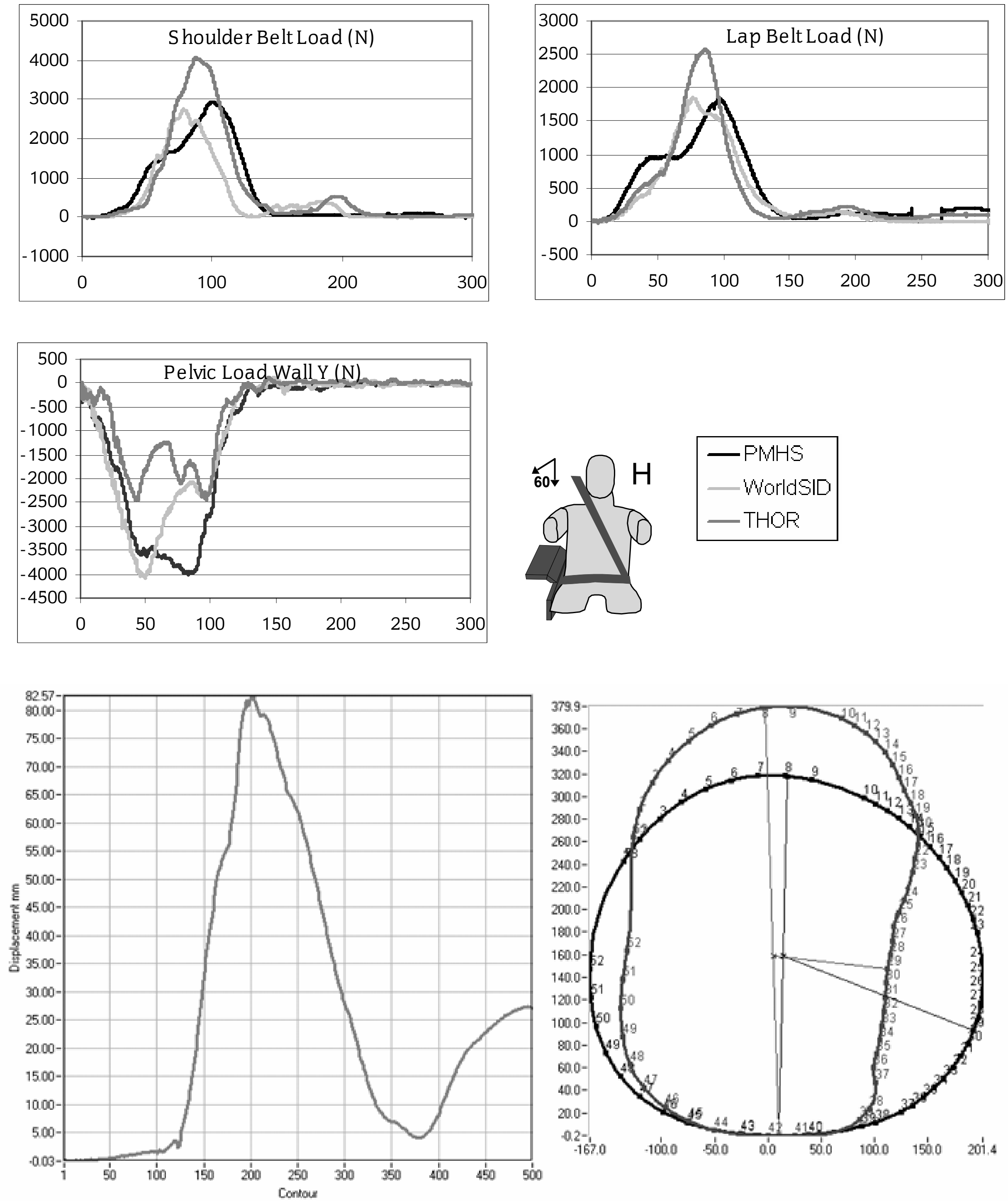

Configuration-15 response curves; high delta-V, 60-degree, inboard shoulder belt, high belt position. Time axis is in milliseconds. Chestband contours are from the PMHS test with "X" marks where equivalent dummy recordings would be.

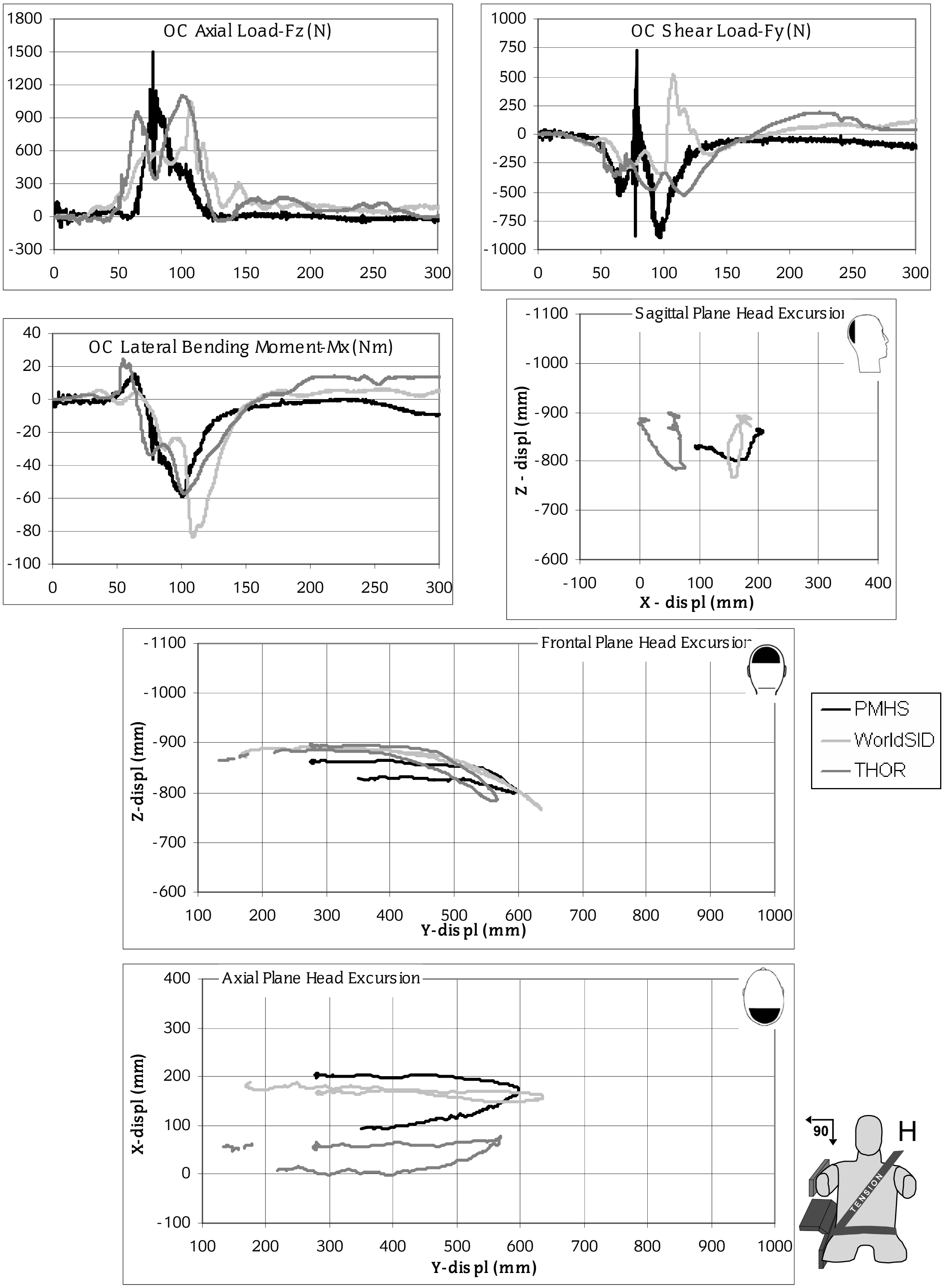

Configuration-16 response curves; high delta-V, 90-degree, shoulder plate, outboard shoulder belt-Pretension. Time axis is in milliseconds. Head excursion measures are relative to seat reference frame.

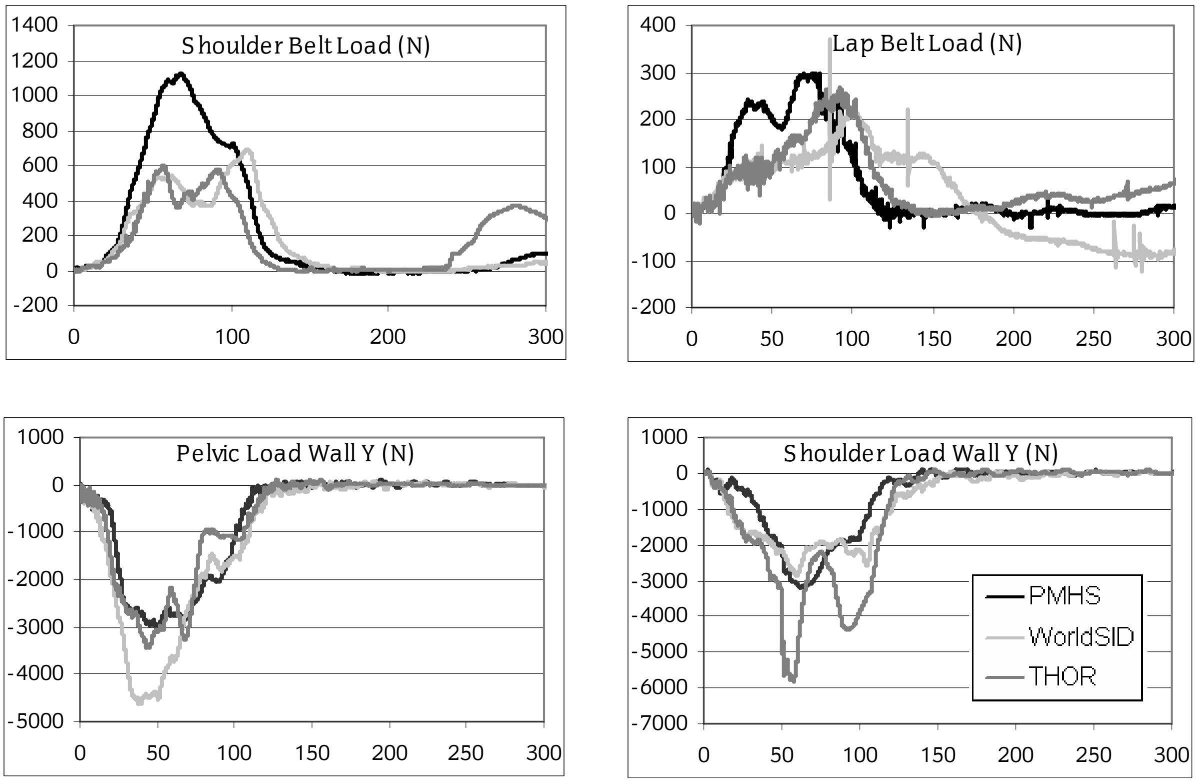

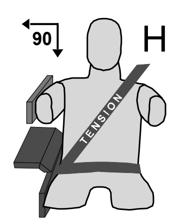

Configuration-16 response curves; high delta-V, 90-degree, shoulder plate, outboard shoulder belt-Pretension. Time axis is in milliseconds.

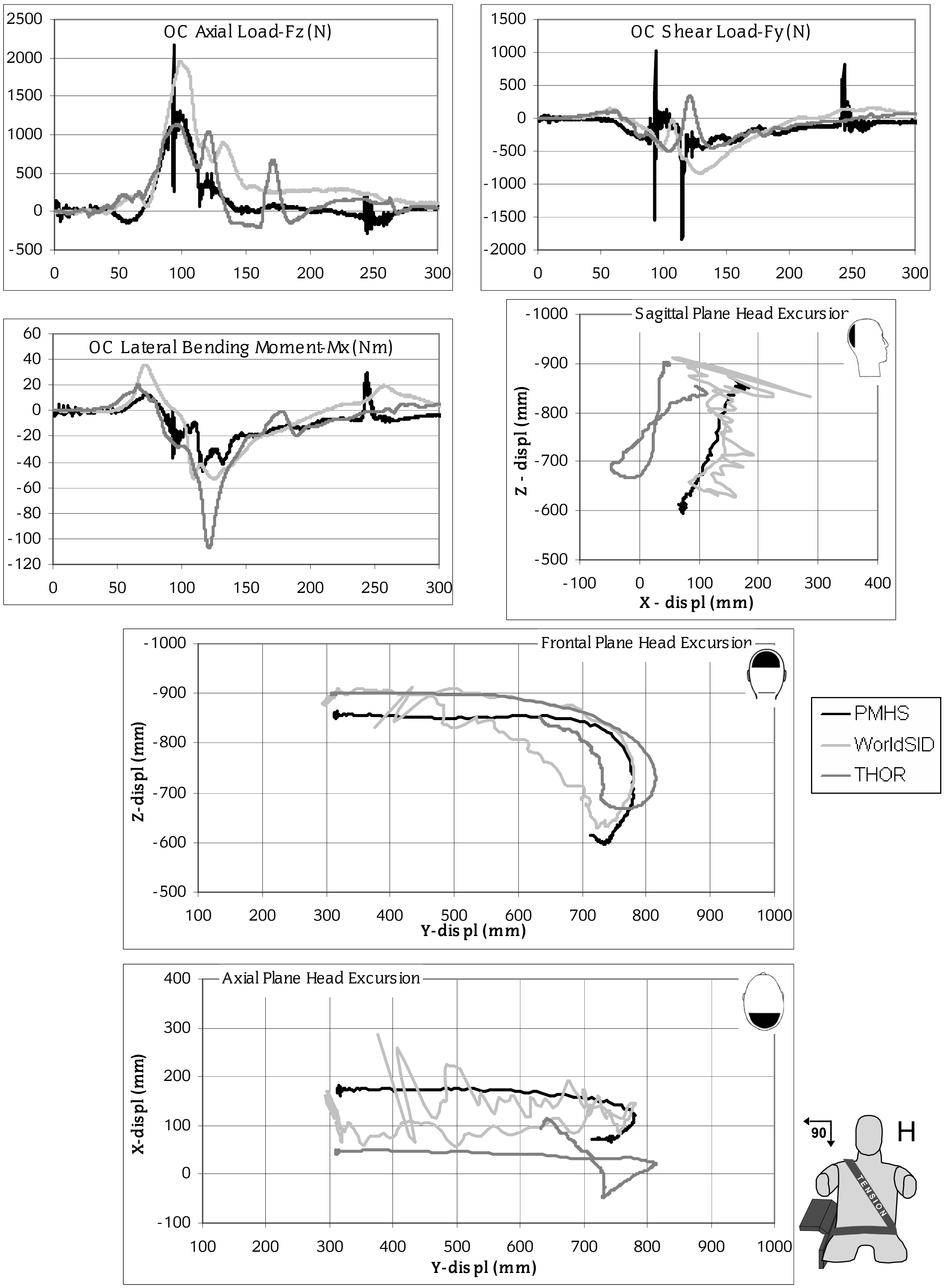

Configuration-18 response curves; high delta-V, 90-degree, inboard shoulder belt, Low belt position-Pretension. Time axis is in milliseconds. Head excursion measures are relative to seat reference frame.

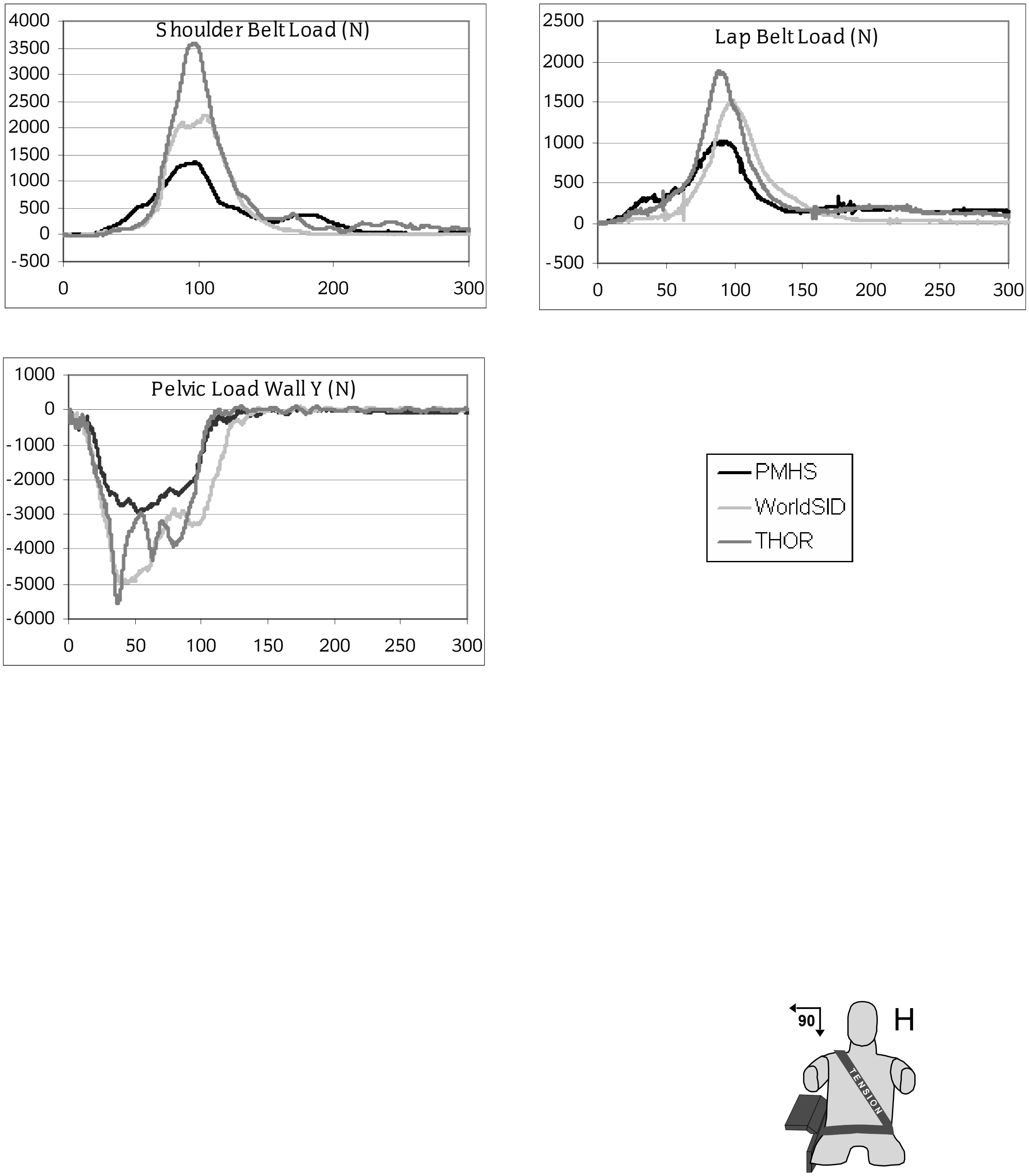

Configuration-18 response curves; high delta-V, 90-degree, inboard shoulder belt, Low belt position-Pretension. Time axis is in milliseconds.

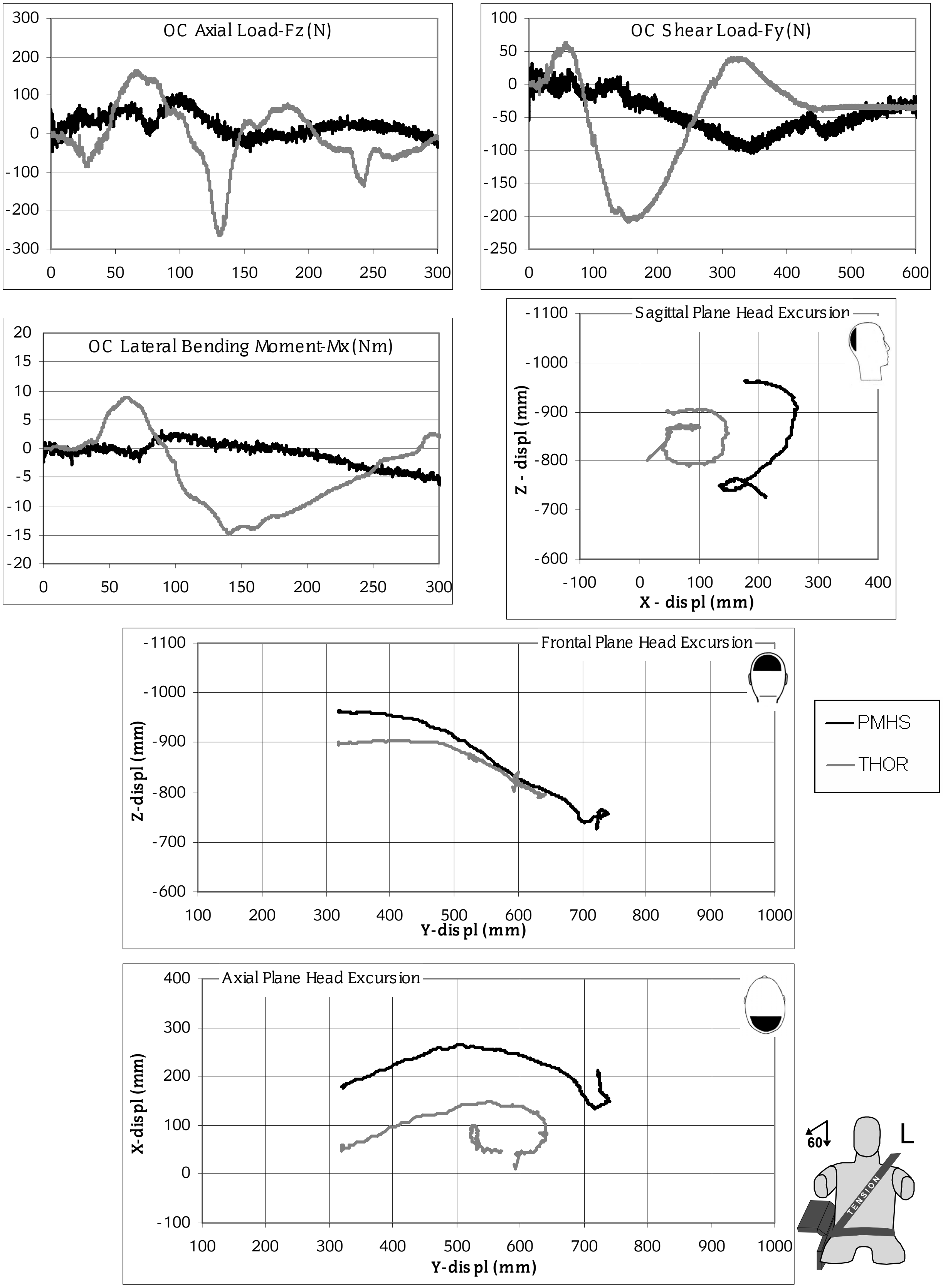

Configuration-20 response curves; low delta-V, 60-degree, outboard shoulder belt-Pretension. Time axis is in milliseconds. Head excursion measures are relative to seat reference frame.

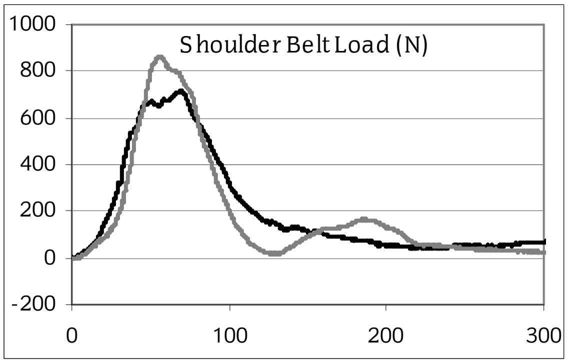

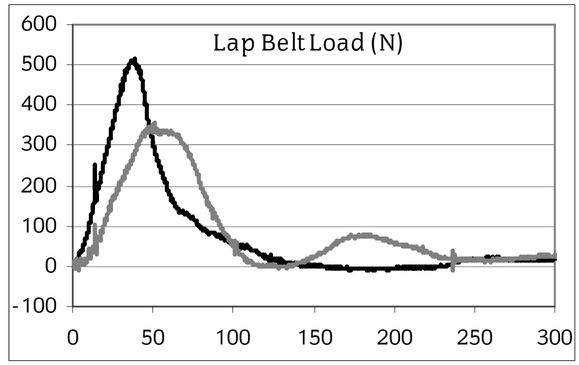

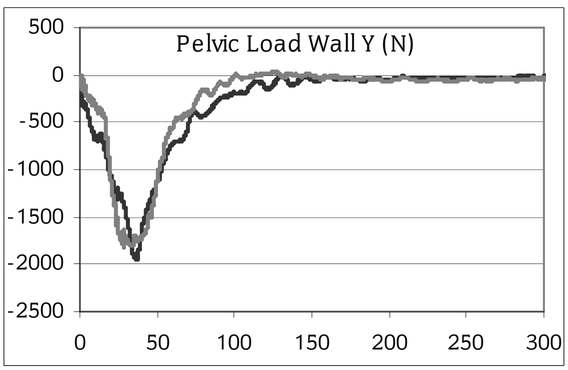

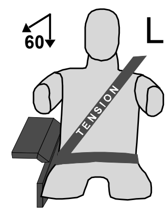

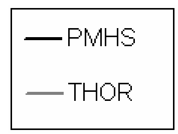

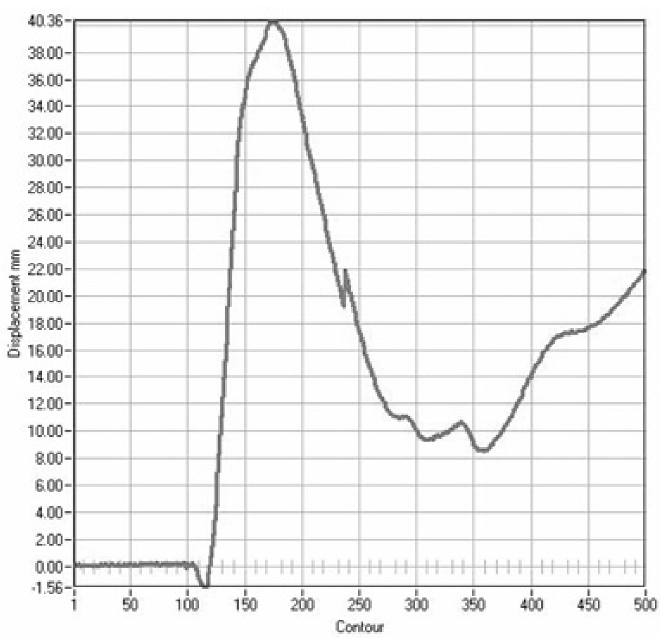

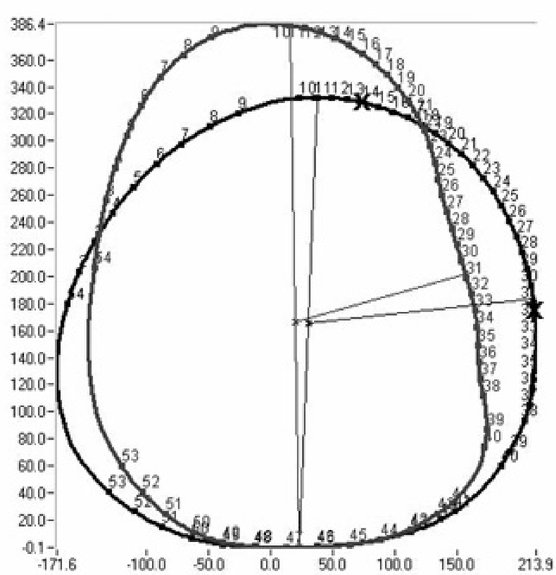

Configuration-20 response curves; low delta-V, 60-degree, outboard shoulder belt-Pretension. Time axis is in milliseconds. Chestband contours are from the PMHS test with “X” marks where equivalent dummy recordings would be.

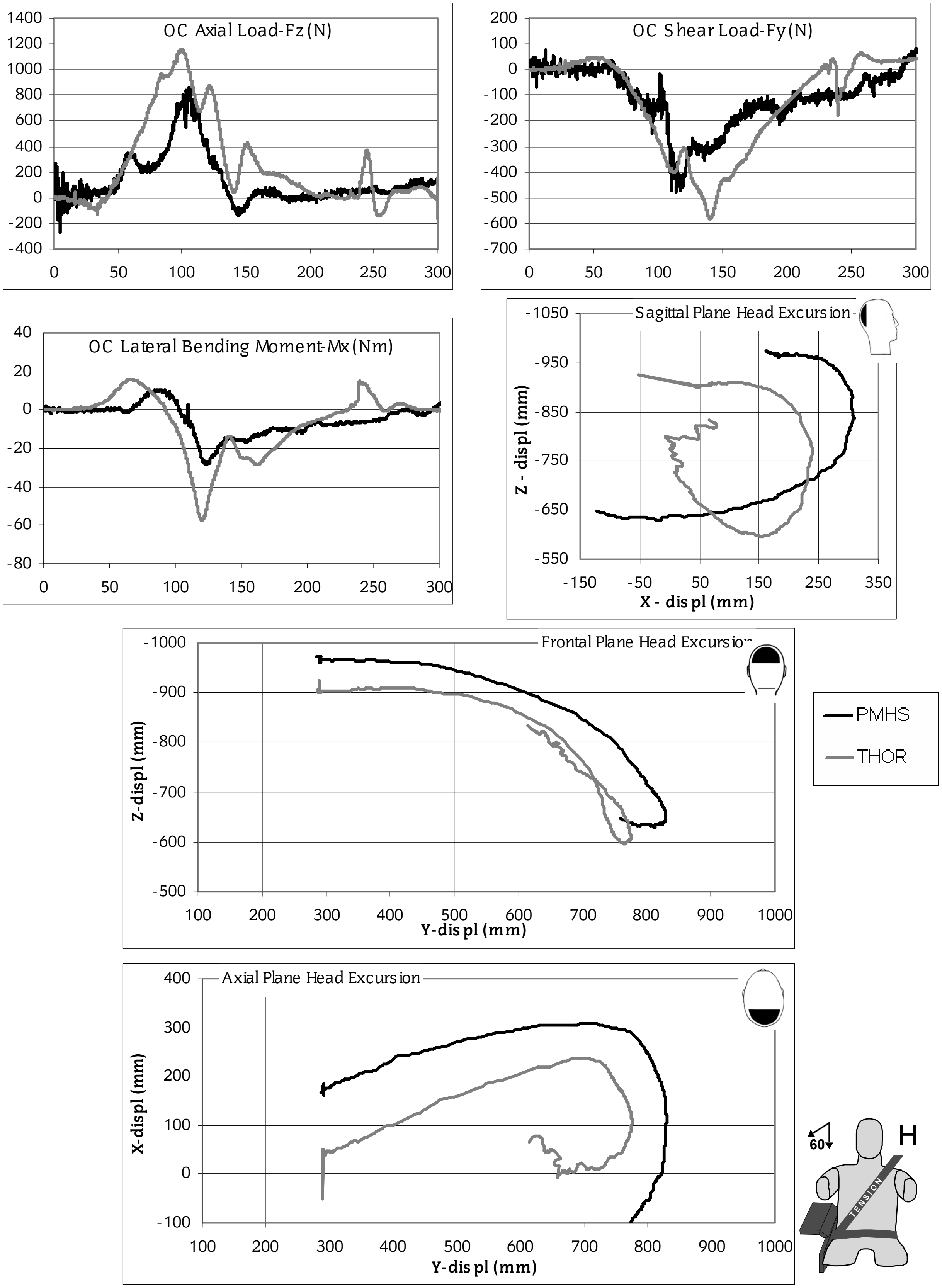

Configuration-21 response curves; high delta-V, 60-degree, outboard shoulder belt-Pretension. Time axis is in milliseconds. Head excursion measures are relative to seat reference frame.

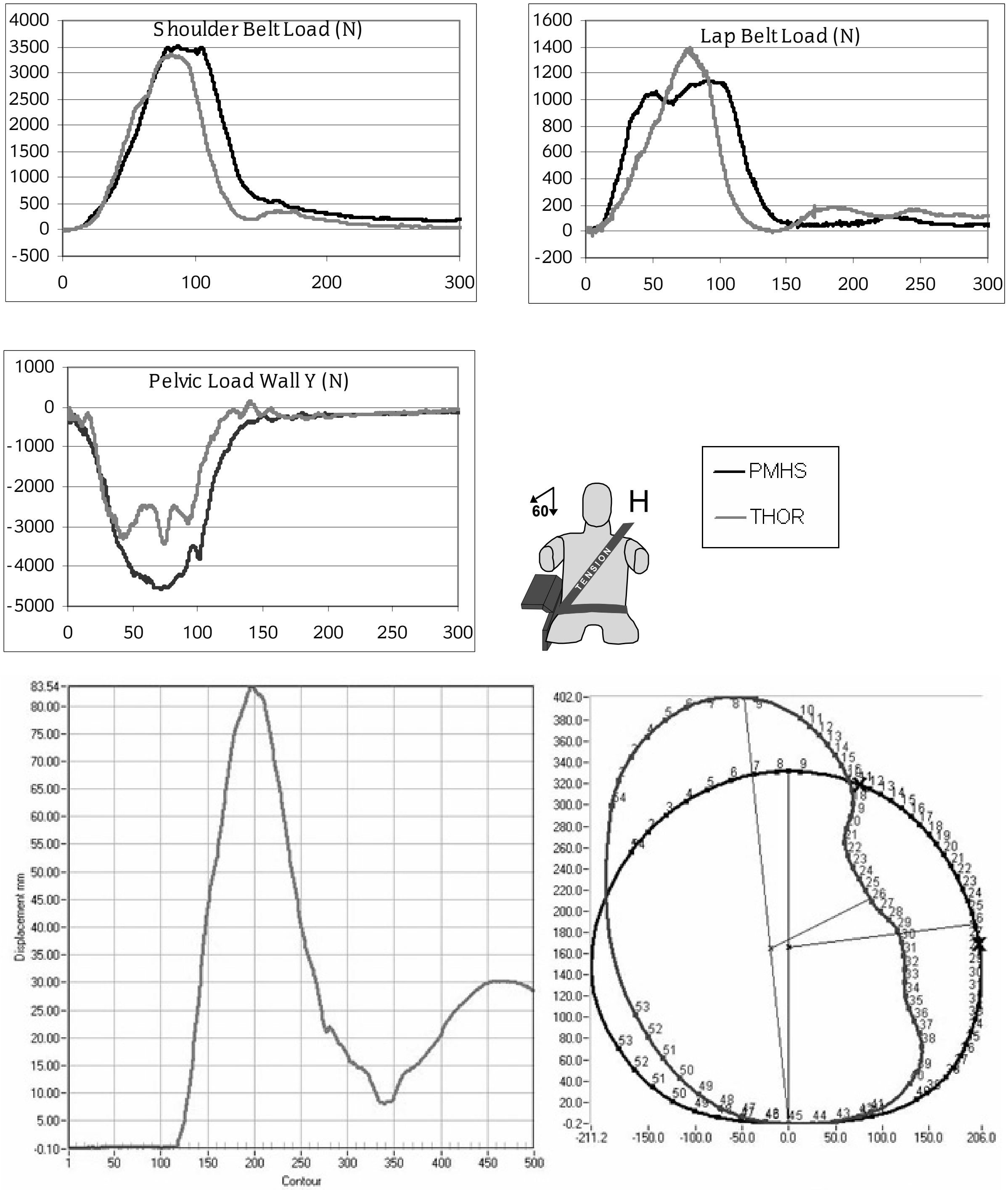

Configuration-21 response curves; high delta-V, 60-degree, outboard shoulder belt-Pretension. Time axis is in milliseconds. Chestband contours are from the PMHS test with "X" marks where equivalent dummy recordings would be.

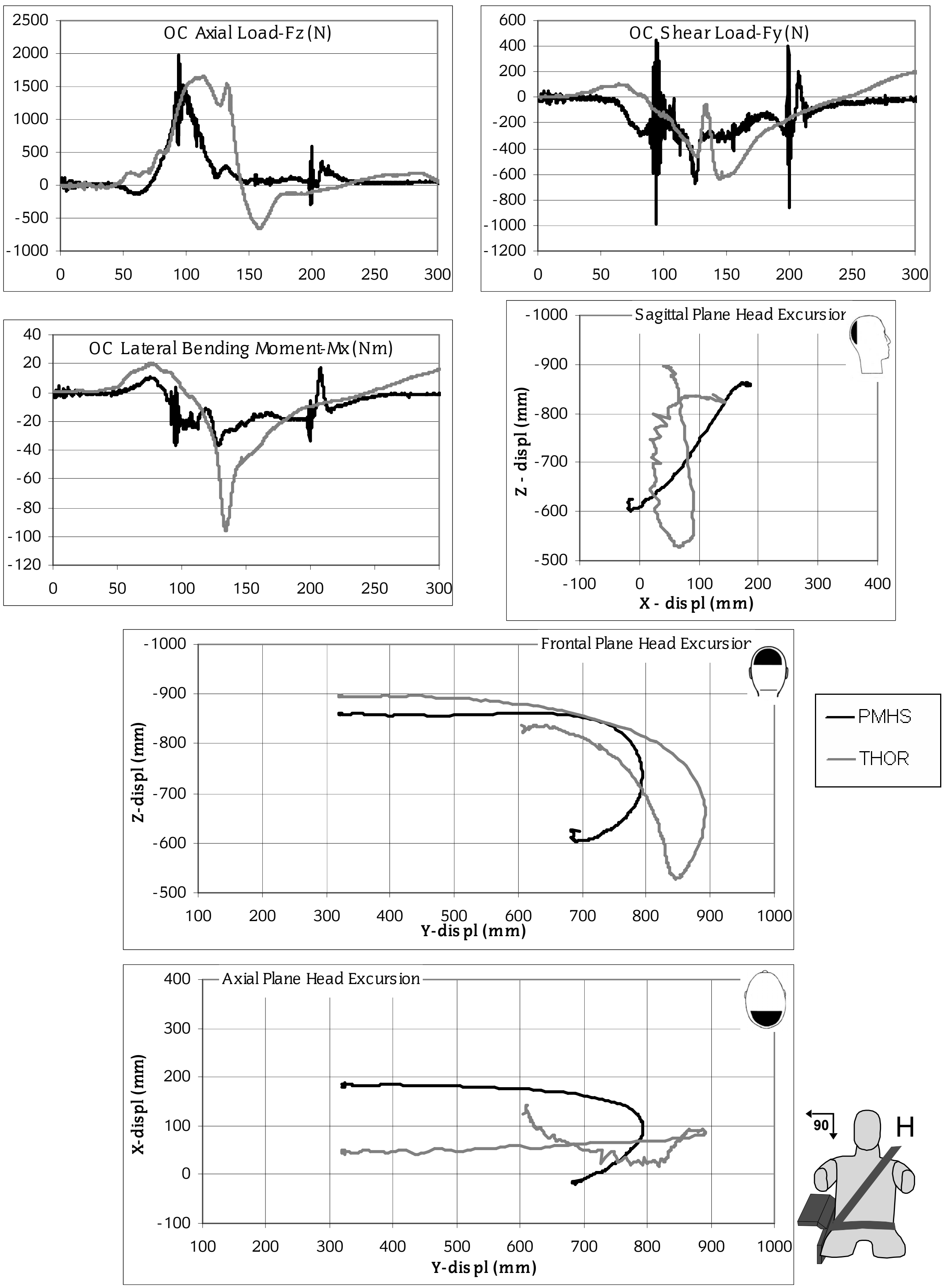

Configuration-22 response curves; high delta-V, 90-degree, outboard shoulder belt. Time axis is in milliseconds. Head excursion measures are relative to seat reference frame.

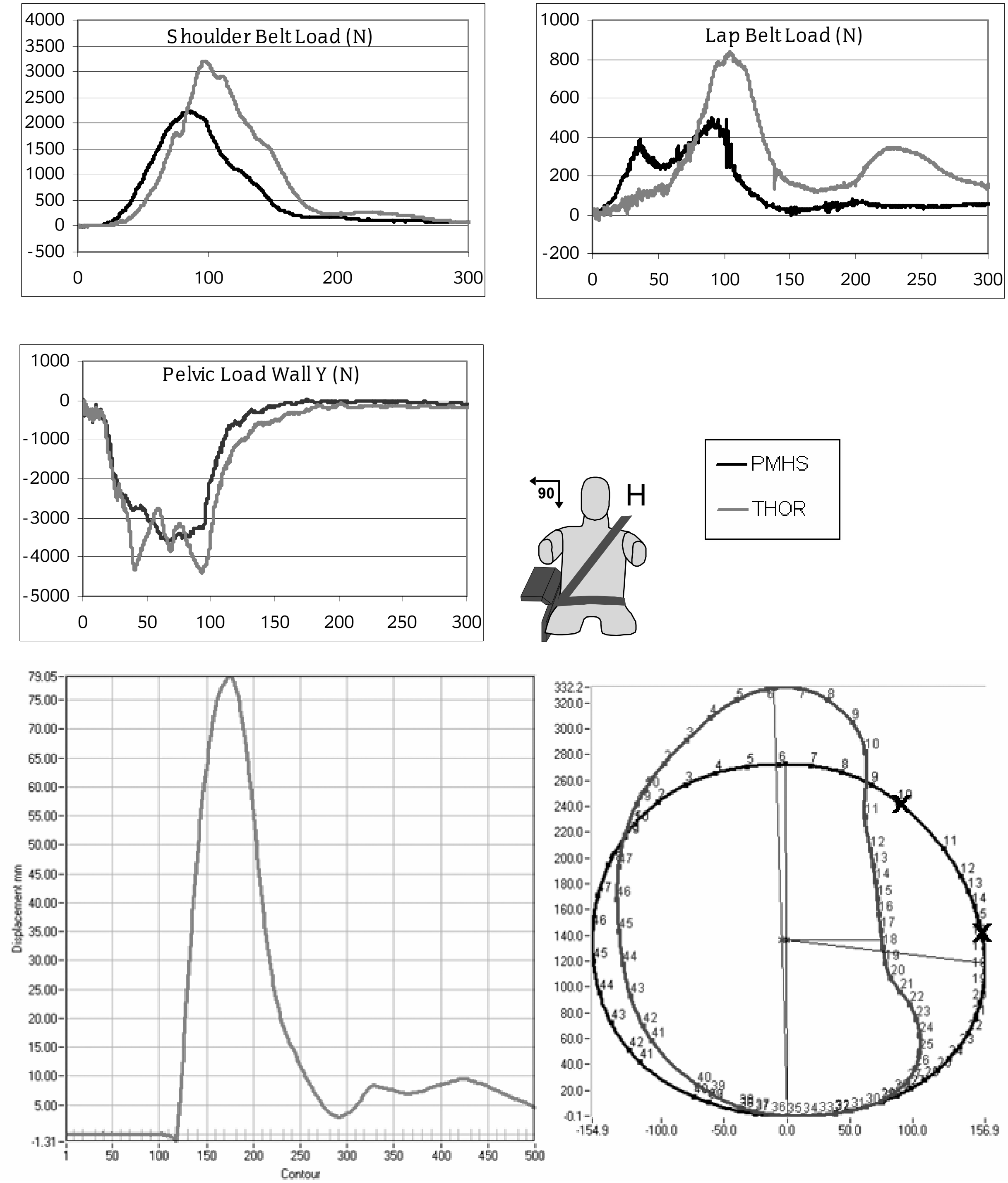

Configuration-22 response curves; high delta-V, 90-degree, outboard shoulder belt. Time axis is in milliseconds. Chestband contours are from the PMHS test with “X” marks where equivalent dummy recordings would be.